AN5964

Application note

99.3% efficiency, 2 kW, 3-channel interleaved totem pole PFC with resonant ZVS digital control

Introduction

Nowadays, in PFC for servers and telecom (for example, PSU for 5G base stations, grid connected smart systems) the achievement of an efficiency >99% is becoming mandatory. The demand for very high efficiency has a strong impact on topologies, design parameters, materials, and control strategies.

The STEVAL-TTPPFC01 offers a very high flat efficiency PFC solution in a full digital three-channel interleaved totem pole topology. A conversion efficiency of 99.3% is obtained using ST MDmesh DM6 superjunction power MOSFETs, as well as a very high power factor and low THDi. The PFC operates in the zero voltage switching (ZVS) resonant mode with hysteresis current control, which is fully implemented in the STM32G474QE microcontroller, thanks to the integrated DACs, fast comparators, and high-resolution timer peripheral HRTIM, to ensure a high dynamic and precise cycle-by-cycle current control.

The STEVAL-TTPPFC01 evaluation kit is a modular solution, which consists of: a power board, which contains all the main passive devices and all the daughter boards plug connectors; a control board, which embeds the STM32G474QE microcontroller; an auxiliary power supply board, which generates all the voltages for driving, sensing, MCU, etc.; three high-frequency half-bridge boards; a low-frequency half-bridge board.

Figure 1. STEVAL-TTPPFC01 board photo

1 Disclaimers for safety

Danger: *Use the STEVAL-TTPPFC01 board only after applying a fire-resistant cover. The cover is not included in the board package.*

There is danger of serious personal injury, property damage or death due to electrical shock and burn hazards if the kit or components are improperly used or installed incorrectly.

Warning: *The kit is not electrically isolated from the high-voltage supply AC-DC input.*

The evaluation board is directly linked to the mains voltage. No insulation is ensured between the accessible parts and the high voltage. All measurement equipment must be isolated from the mains before powering the board.

When using an oscilloscope with the evaluation board, it must be isolated from the AC line.

This prevents shock from occurring as a result of touching any single point in the circuit, but does NOT prevent shock when touching two or more points in the circuit.

Caution: During assembly, testing, and operation, the evaluation board poses several inherent hazards, including bare wires, moving or rotating parts and hot surfaces. All operations involving transportation, installation, use and maintenance must be performed by skilled technical personnel who is familiar with the installation, use and maintenance of power electronic systems.

Work area safety:

The work area must be clean and tidy.

Do not work alone when boards are powered.

Protect the area against any unauthorized access by putting suitable barriers and signs.

A system architecture that supplies power to the evaluation board must be equipped with additional control and protective devices in accordance with the applicable safety requirements (i.e., compliance with technical equipment and accident prevention rules).

Electrical safety:

Arrange measurement setup, wiring, and configuration, paying attention to the high voltage section. Once the setup is complete, power the board. Fuse protection is included with this evaluation board.

Danger: *Do not touch the evaluation board when it is powered or immediately after it has been disconnected from the voltage supply as several parts and power terminals containing potentially energized capacitors need time to discharge, and heat-sinks and transformers may still be very hot.*

Personal safety:

Always wear suitable personal protective equipment, such as insulating gloves and safety glasses.

Take adequate precautions and install the board preventing accidental touch.

Use protective shields, such as insulating box with interlocks.

2 System overview

The STEVAL-TTPPFC01 incorporates the following design features to achieve above 99% efficiency:

- **Bridgeless topology**: the large input bridge losses of conventional PFCs (diode forward voltage losses) are dramatically reduced thanks to the use of active switches for the mains rectification function ($R_{ds\ (on)}$ losses in a MOSFET).
- **Interleaved architecture**: thanks to the phase shedding (enabling/disabling the parallel channels basing on the load requirement) the light load efficiency is improved and a flat efficiency over the whole load range is obtained. Moreover, the superposition of the inductor currents of each boost cell results in a smooth mains current waveform (EMI filter and inductors volume reduction) and output capacitor loss reduction (lower equivalent inductor current ripple).
- **Zero voltage switching (ZVS) resonant technique**: eliminates the turn-on losses of the power switches over the full mains period to further improve converter efficiency.

2.1 Block diagram

The STEVAL-TTPPFC01 implements ZVS-PFC control with the STM32G474 microcontroller. It includes:

- The slow outer voltage loop: for the output voltage regulation (green dashed rectangle)
- The faster inner current loop: for the inductor currents control (red dashed rectangle)
- The input rectification function: for the mains synchronization (blue dashed rectangle)

The output voltage is regulated to its reference value with standard PI regulator, which calculates the PFC input peak current value I_{pk}. The current reference generator will provide the peak current references (I_{F1}, I_{F2}, I_{F3}) to manage the current sharing among the three high-frequency cells based on the load requirement. Moreover, a fast input and load feedforward is included to enhance the PFC dynamic response if a load step or an input voltage variation occurs.

Figure 2. **STEVAL-TTPPFC01 block diagram**

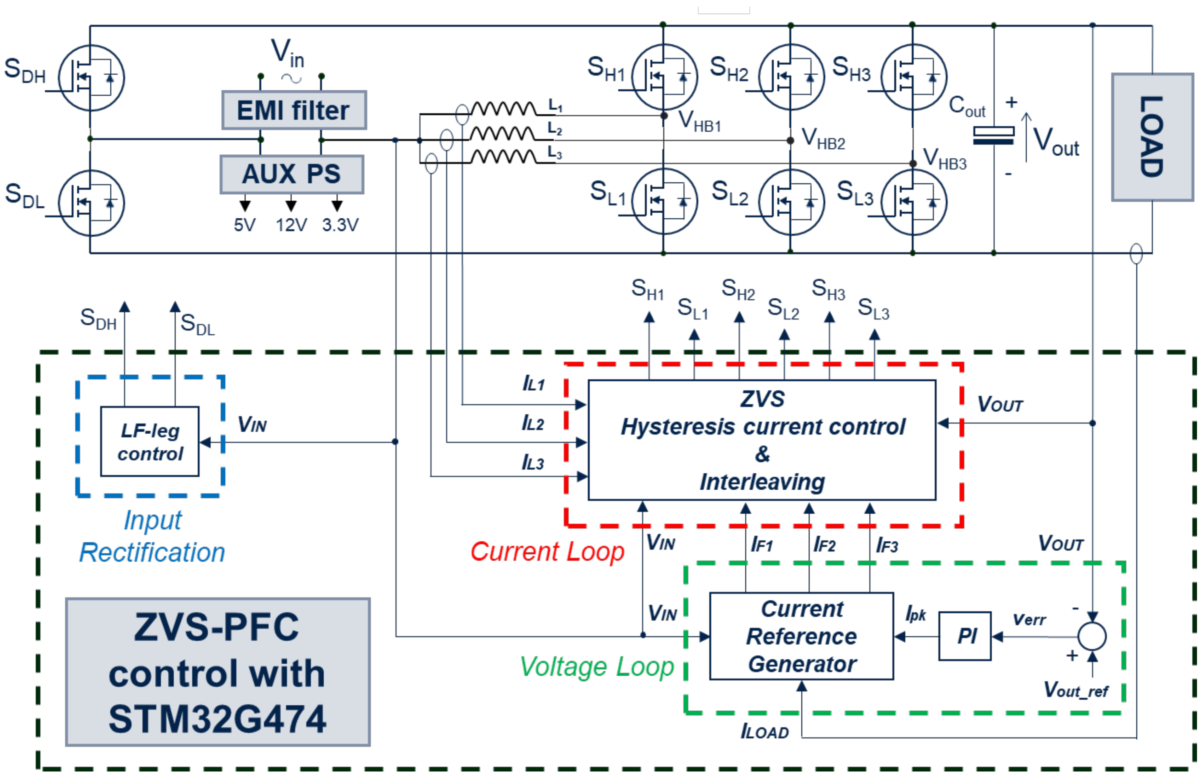

The sophisticated and high performance inner current loop is a hysteresis current control implemented with internal DACs, fast comparators, and the powerful high-resolution timers (HRTIM) peripheral of the STM32G474QE [1]. Thus, the highest possible bandwidth and cycle-by-cycle regulation are ensured for the inductor currents.

Finally, the STEVAL-TTPPFC01 doesn't require any external bias since an auxiliary power supply (AUX PS) is included to generate the voltages for MCU, sensing and driving circuits, hence the presence of input mains voltage (V_{in}) is enough to run the board.

2.2 ZVS-PFC operation

In Figure 3, a single cell of the totem pole PFC is shown together with the ZVS switching waveforms.

The power switches S_{DH} and S_{DL} (low-frequency leg) perform the mains rectification at the line frequency, while S_L and S_H (high-frequency legs) are driven at high frequency to shape the inductor current, as described in [2].

ZVS operation is performed exploiting the resonance between the boost inductance L and equivalent output capacitance of the MOSFET $C=C_{ossH}//C_{ossL}$. The low-side MOSFET S_L is closed until I_L reaches the peak value $+I_F*$, then S_L is turned-off and the positive resonance. The midpoint voltage V_{HB} reaches the V_{out} value after the time t_{Vout_Vds}, hence the high-side MOSFET S_H is closed in ZVS condition. When I_L reaches the negative value I_R*, S_H is turned-off and the negative resonance between L and C leads V_{HB}=0, hence S_L is turned-on after t_{zero_Vds}, again in ZVS condition. The condition V_{HB}=0 is ensured only if the additional charge related to negative inductor current is enough to completely discharge equivalent output capacitance C of the MOSFET.

Figure 3. Single cell totem pole bridgeless PFC with ZVS waveforms

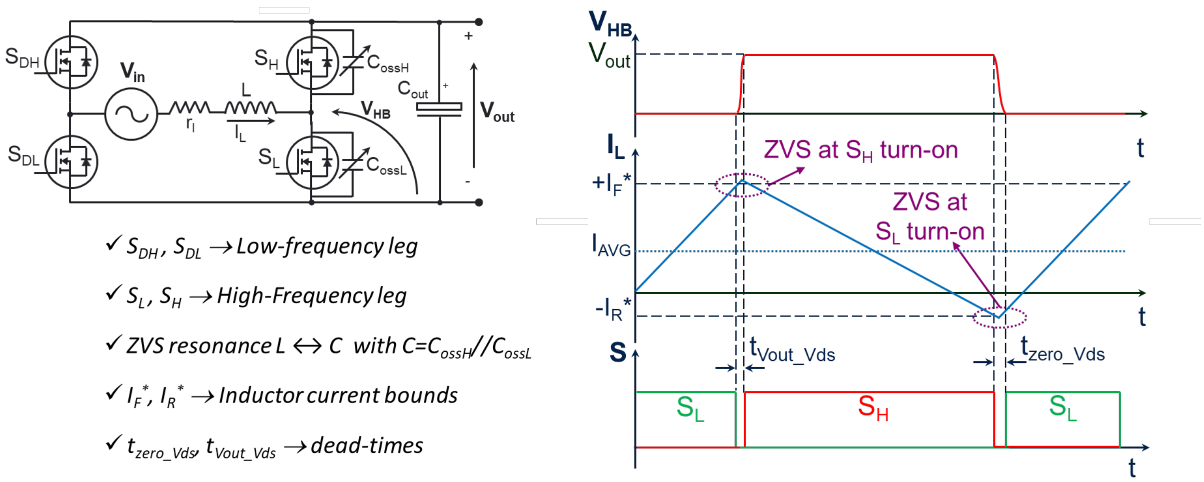

Consequently, the high threshold I_F*, low threshold I_R* and the dead times t_{Vout_Vds} and t_{zero_Vds} are obtained solving the equations that describe the L-C resonance transient:

$$\begin{cases} s^2 + 2\alpha s + \omega_0^2 = 0 \\ v_C(t) = C_1 e^{-\alpha t}(\cos\beta t + \varphi_1) + V_C(\infty) \\ i_L(t) = C_2 e^{-\alpha t}(\cos\beta t + \varphi_2) + I_L(\infty) \end{cases} \quad (1)$$

Where $v_{HB}(t)=v_c(t)$, $V_C(\infty)=V_{IN}$ and $I_L(\infty)=0$.

ω_0 is the angular resonance frequency, β is the imaginary part of the solution while the real part is given by the attenuation factor α, which is proportional to the inductor series resistance r_l:

$$\begin{cases} \alpha = \frac{r_l}{2L} \\ \beta = \sqrt{\omega_0^2 - \alpha^2} \\ \omega_0^2 = \frac{1}{LC} \end{cases} \quad (2)$$

For a better understanding, the comparison between ZVS and TM-QR (transition mode quasi-resonant) is show in Figure 4. The typical capacitive losses P_{cap} (turn-on losses) of TM-QR are eliminated in the ZVS operation because the MOSFETs are always turned-on when the drain-source voltage is equal to zero, $V_{ds}=V_{HB}=0$, as illustrated in Figure 3.

Figure 4. **Comparison between TM-QR and ZVS operations**

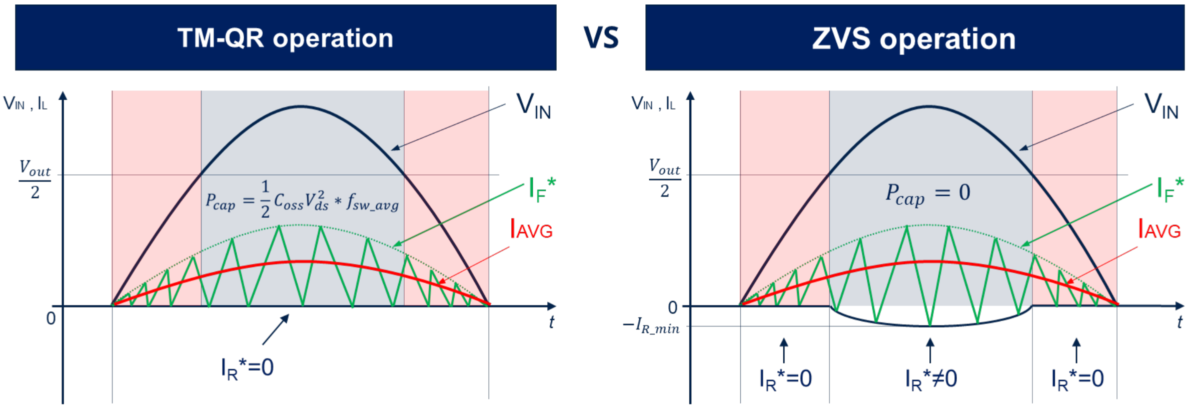

For $V_{in} \leq V_{out}/2$ the MOSFET equivalent capacitance is naturally discharged by itself during the resonance transition, hence a reverse inductor current I_R* is required only for $V_{in}>V_{out}/2$. Among several possible choices (theoretically infinite), the minimum value of reverse inductor current $I_R*=I_{R\_min}$, which ensures the ZVS, is selected to minimize the rms current in the switches and the inductor, with the related copper losses.

To obtain a more realistic view, Figure 5 shows the simulated behavior of the inductor current and the switching frequency during the positive half-line cycle of the input voltage ($V_{in}>0$):

Figure 5. Typical I_L and f_{sw} behavior for ZVS-PFC at V_{in}=230 Vac, V_{out}=390 Vdc

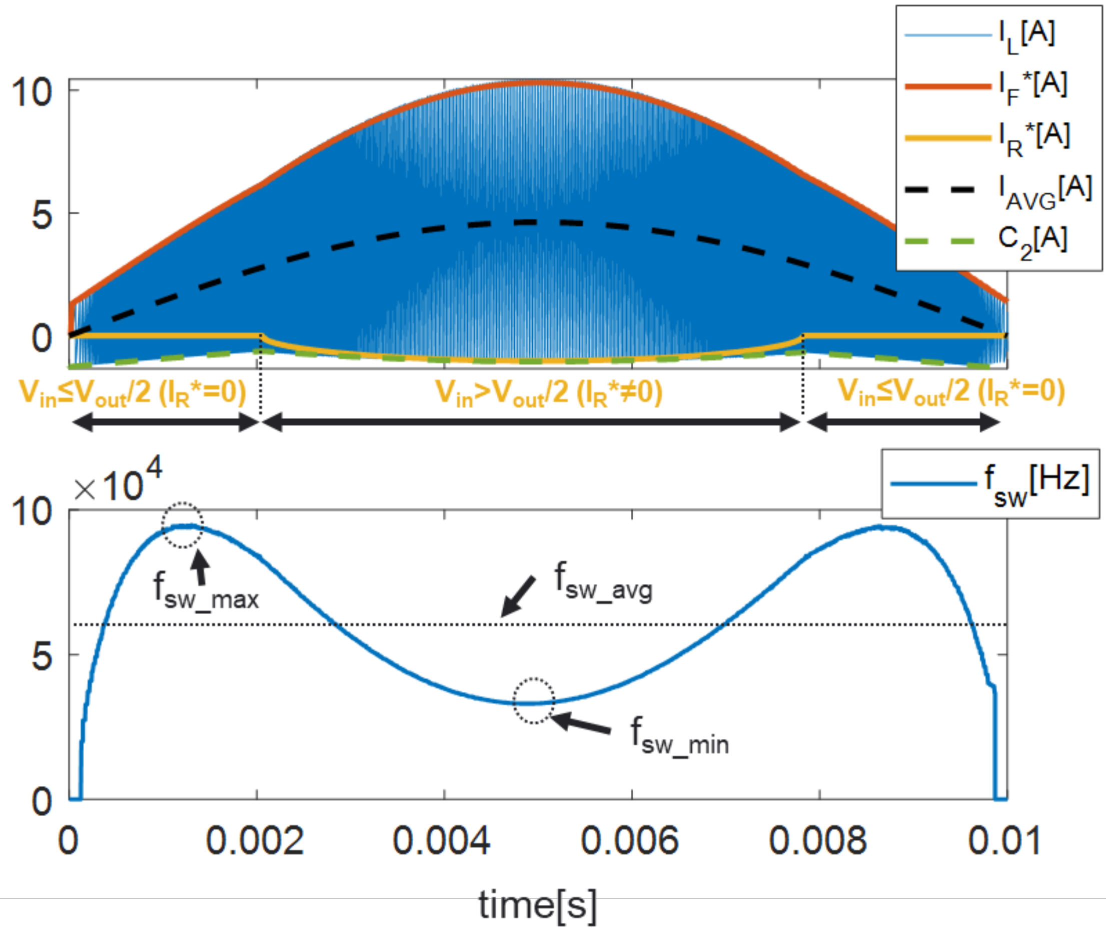

3 Power stage design

This section shows the criteria adopted to select the main power stage components according to the board specifications in the following table.

Table 1. STEVAL-TTPPFC01 design specifications

Parameter	Value
Input voltage (V_{in})	90-253 Vac, 47-63 Hz
Output voltage (V_{out})	390 Vdc
Target efficiency (η)	≥99% at 230Vac and full load
Output power (P_{out})	2 kW at V_{in}≥207 Vac, 1 kW at V_{in}=115 Vac
Target power factor (PF)	≥0.99 at 230Vac and full load
Variable switching frequency (f_{sw})	(24-300) kHz
Hold-up time (t_{hold_up})	10 ms at $V_{out\ (\ MIN)}$=350 Vdc
Output voltage ripple	5% of V_{out} at full load

Since the aim of STEVAL-TTPPFC01 design is to reach the target efficiency of ≥99% at nominal voltage, the value V_{in} = 230 Vac is used in loss estimation and maximum device temperature of 50°C is assumed. Due to the saturation limit of the boost inductors, the maximum power managed by STEVAL-TTPPFC01 is derated at V_{in} = 207 Vac (see Figure 8).

3.1 Mains rectifier switch

The PFC input current is evaluated at 230 Vac input voltage and 2 kW output power (full load):

$$I_{in\_rms} = \frac{P_{out}}{\eta \cdot V_{in\_rms} \cdot PF} = \frac{2000}{0.99 \cdot 230 \cdot 0.99} = 8.87A \quad (3)$$

As there are only the conduction losses in the low frequency leg, the STY145N65M5 [3] is selected to perform the input voltage rectification because of its very low R_{DSon} (max 15 mΩ). Hence, the conduction losses are calculated for the target temperature of 50°C:

$$P_{tot\_LF} = R_{on(50°C)} \cdot I_{in_{rms}}^2 = 1.25 \cdot 0.015 \cdot 8.87^2 = 1.47W \quad (4)$$

3.2 Boost inductor

The resonant ZVS operation mode can be seen as an extension of the TM-QR (also called critical conduction mode, CrM) where a negative inductor current is applied for a portion of the input voltage (V_{in}≥V_{out}/2), as shown in Figure 4. Hence, to simplify the boost inductor design, the TM equations of [4] can be used as first approximation to provide the manufacturing specs and determinate the switching frequency of the converter.

As the inductor current is a triangular waveform (modulated with V_{in} sinusoidal amplitude), the maximum peak of the inductor current is twice the maximum line-frequency peak current evaluated at the derating voltage V_{in} = 207 Vac:

$$IL_{pk} = \frac{2 \cdot \sqrt{2} \cdot I_{in\_rms(Vin\_rms\_der)}}{N_{ch}} = \frac{2 \cdot \sqrt{2} \cdot 9.86}{3} = 9.3A \quad (5)$$

A saturation current of 14 A is a good choice for the inductor to have enough margin for PFC regulation, especially during transients, also considering a typical inductor tolerance of ±15%.

The RMS inductor current is calculated as:

$$IL_{rms} = \frac{2 \cdot I_{in\_rms(Vin\_rms\_der)}}{\sqrt{3} \cdot N_{ch}} = \frac{2 \cdot 9.86}{\sqrt{3} \cdot 3} = 3.8A \quad (6)$$

Finally, the inductor value is set to meet the minimum switching frequency requirement of 24 kHz. The evaluation is done both at minimum and maximum input voltage (at full load), then the minimum between the two values is selected:

$$L = \frac{V_{in\_rms}^2 \cdot \left(V_{out} - \sqrt{2} \cdot V_{in\_rms}\right)}{2 \cdot f_{sw\_min} \cdot \eta \cdot P_{out} \cdot V_{out}} \tag{7}$$

$$L\left(V_{in\_rms\_min}\right) = \frac{207^2 \cdot \left(390 - \sqrt{2} \cdot 207\right)}{2 \cdot 24000 \cdot 0.99 \cdot 2000 \cdot 390} = 327\ \mu H \tag{8}$$

$$L\left(V_{in\_rms\_max}\right) = \frac{253^2 \cdot \left(390 - \sqrt{2} \cdot 253\right)}{2 \cdot 24000 \cdot 0.99 \cdot 2000 \cdot 390} = 162\ \mu H \tag{9}$$

$$L \leq \min\left[L\left(V_{in\_rms\_min}\right), L\left(V_{in\_rms\_max}\right)\right] \tag{10}$$

Thus, for this application 160 µH inductor has been selected.

3.3 Input capacitor

The input capacitor must filter the high frequency voltage ripple generated by the input current ripple. A polypropylene film capacitor, rated for maximum input voltage, is recommended. The formula is:

$$C_{in} = \frac{\frac{k_r}{N_{ch}} \cdot I_{in\_rms(Vin\_rms\_max)}}{2\pi \cdot f_{sw(Vin\_pk)} \cdot r \cdot V_{in\_rms\_max}} = \frac{\frac{1.2}{3} \cdot 8.06}{2\pi \cdot 24000 \cdot 10^3 \cdot 0.02 \cdot 253} = 4.23\mu F \tag{11}$$

Where

k_r = inductor current ripple factor (it is >1 due to the applied reverse inductor current I_R*)

r = maximum high frequency voltage ripple factor ($\Delta V_{IN}/V_{IN}$ = 2-10%)

$f_{sw(Vin\_pk)}$ = switching frequency at the peak value of the input voltage

N_{ch} = number of interleaved channels

Finally, a 4.7 µF input capacitor is used in this design.

3.4 Output capacitor

Usually two criteria are applied, at rated power, for output capacitor selection. The PFC output voltage ripple ΔV_{out} at twice of line frequency must be within the specified target value (5% of V_{out} in this design):

$$C_{out\_R} \geq \frac{P_{out}}{2\pi \cdot f_{line} \cdot \Delta V_{out} \cdot V_{out}} = \frac{2000}{2\pi \cdot 50 \cdot 19.5 \cdot 390} = 837\mu F \tag{12}$$

Moreover, after a line interruption of a defined duration (hold-up time t_{hold_up}) the PFC output voltage must remain higher than the minimum allowable target value $V_{out\ (MIN)}$:

$$C_{OUT\_H} \geq \frac{2 \cdot P_{out} \cdot t_{hold\_up}}{\left(V_{out} - \frac{\Delta V_{out}}{2}\right)^2 - V_{out(MIN)}^2} = \frac{2 \cdot 2000 \cdot 10 \cdot 10^{-3}}{\left(390 - \frac{19.5}{2}\right)^2 - 350^2} = 1810\mu F \tag{13}$$

Finally, the maximum capacitance value between the two criteria is selected to meet both requirements:

$$C_{OUT} \geq \max\left(C_{OUT\_R}, C_{OUT\_H}\right) = 1810\mu F \tag{14}$$

Hence, we use 6 x 330 µF capacitors in parallel in this design.

3.5 Low-side power switch

To evaluate switch RMS currents in the high-frequency leg of the totem pole topology are evaluated for the positive half-line cycle (V_{in}>0), hence the low-side switch works as boost rectifier:

$$I_{LS\_rms} = IL_{pk(Vin\_rms)}\sqrt{\frac{1}{6} - \frac{4 \cdot V_{in\_rms} \cdot \sqrt{2}}{9 \cdot \pi \cdot V_{OUT}}} = 8.36\sqrt{\frac{1}{6} - \frac{4 \cdot 230 \cdot \sqrt{2}}{9 \cdot \pi \cdot 390}} = 1.85A \tag{15}$$

For this application, an MDmesh DM6 MOSFET is used as the boost switch. Compared with the previous generation fast MDmesh, DM6 combines very low recovery charge (Q_{rr}), recovery time (t_{rr}) and excellent improvement in $R_{DS(on)}$ per area with one of the most effective switching behaviors available on the market for the most demanding high-efficiency topologies and ZVS phase-shift converters. The STW70N60DM6 [5] has been selected for this design and the conduction loss is evaluated at 50°C:

$$P_{cond\_HF\_LS} = R_{on(50°C)} \cdot I^2_{LSrms} = 1.25 \cdot 0.036 \cdot 1.85^2 = 0.154W \quad (16)$$

The turn-on loss is eliminated thanks to the ZVS resonant technique, while the turn-off loss can be calculated basing upon the average peak current and switching frequency in one half-line cycle and the estimated fall time:

$$I_{LS\_pk\_avg} = I_{Lpk,avg} = \frac{2 \cdot IL_{pk(Vin\_rms)}}{\pi} = \frac{2 \cdot 8.36}{\pi} = 5.32A \quad (17)$$

$$t_{fall} = C_{iss} \cdot R_g \cdot \ln\left(\frac{V_{pl}}{V_{th}}\right) + C_{rss} \cdot R_g \cdot \left(\frac{V_{ds} - V_{pl}}{V_{pl}}\right) = 4360 \cdot 10^{-12} \cdot 6.2 \cdot \ln\left(\frac{6.3}{4}\right) + 13 \cdot 10^{-12} \cdot 6.2 \cdot \ln\left(\frac{390 - 6.3}{6.3}\right) = 12.61ns \quad (18)$$

$$P_{\mathrm{off\_HF\_LS}} = 0.5 \cdot I_{Lpk,avg} \cdot V_{out} \cdot t_{fall} \cdot f_{\mathrm{sw\_avg}} = 0.5 \cdot 5.32 \cdot 390 \cdot 12.61 \cdot 10^{-9} \cdot 60 \cdot 10^3 = \ = 0.773\ W \quad (19)$$

Where:

C_{iss} = Input capacitance

C_{rss} = Reverse transfer capacitance

R_g = Sum of intrinsic (internal) and external gate resistance

V_g = Gate-source driving voltage

V_{th} = Gate-source threshold voltage

V_{pl} = Plateau voltage

V_{ds} = Drain-source voltage

Due to the nonlinear output capacitance of the MOSFET, C_{oss}, the turn-off losses could be lower than calculated by equation (19). Finally, the gate drive loss depends on the total gate charge of the switch Q_g:

$$P_{g\_LS} = V_g \cdot Q_g \cdot f_{sw\_avg} = 12 \cdot 99 \cdot 10^{-9} \cdot 60 \cdot 10^3 = 0.071W \quad (20)$$

3.6 High-side power switch

For V_{in}>0 the high-side switch works as boost rectifier hence the RMS current is:

$$I_{HS\_rms} = IL_{pk(Vin\_rms)}\sqrt{\frac{4 \cdot V_{in\_rms} \cdot \sqrt{2}}{9 \cdot \pi \cdot V_{out}}} = 8.36\sqrt{\frac{4 \cdot 230 \cdot \sqrt{2}}{9 \cdot \pi \cdot 390}} = 2.87A \quad (21)$$

Hence, the conduction losses are estimated at 50°C:

$$P_{cond\_HF\_HS} = R_{on(50°C)} \cdot I^2_{\mathrm{HS\_rms}} = 1.25 \cdot 0.036 \cdot 2.87^2 = 0.371W \quad (22)$$

In this case, the turn-off losses can be neglected as they occur at zero or very low value of negative current (reverse inductor current I_R*). So, at the end, the only high-frequency contribution is given by the driving losses:

$$P_{g\_HS} = P_{g\_LS} = 0.071W \quad (23)$$

3.7 Power loss requirements

The losses estimation in the passive components could be quite difficult and sometimes the adopted approximations are not acceptable, especially when an extreme conversion efficiency is a target design, as in the case of the STEVAL-TTPPFC01. For this reason, in this design the active losses are estimated, to carry out the selection of the switches, while the minimum allowed passive losses are set as target to reach the desired efficiency.

In bridgeless totem pole topology the power dissipated for each device, in the low-frequency leg, is related to one half of the mains period, hence:

$$P_{single\_LF} = \frac{P_{cond\_LF\_tot}}{2} = 0.73W \quad (24)$$

Also, in the high-frequency leg both the low-side and high-side devices will alternate operation as boost or rectifier each half-line cycle. Consequently, the contribution of the conduction and turn-off losses on the single device are obtained by the following equations:

$$P_{cond\_HF\_single} = \frac{\left(P_{cond\_HF\_LS} + P_{cond\_HF\_HS}\right)}{2} = \frac{(0.154 + 0.371)}{2} = 0.262W \quad (25)$$

$$P_{off\_HF\_single} = \frac{P_{off\_HF\_LS}}{2} = \frac{0.773}{2} = 0.386W \quad (26)$$

Hence, the power loss for each high-frequency switch is:

$$P_{single\_HF} = P_{cond\_HF\_single} + P_{off\_HF\_single} + P_{g\_LS} = (0.262 + 0.386 + 0.071) = 0.72W \quad (27)$$

The total power loss of the MOSFETs is obtained by multiplying the single contribution for the total number of switches. Hence, for the STEVAL-TTPPFC01 two switches are considered for the low-frequency leg and six switches for the high-frequency legs.

The maximum allowed loss for passive and all other components is shown in the following figure.

Figure 6. Max allowed losses for STEVAL-TTPPFC01 to meet ≥99% efficiency.

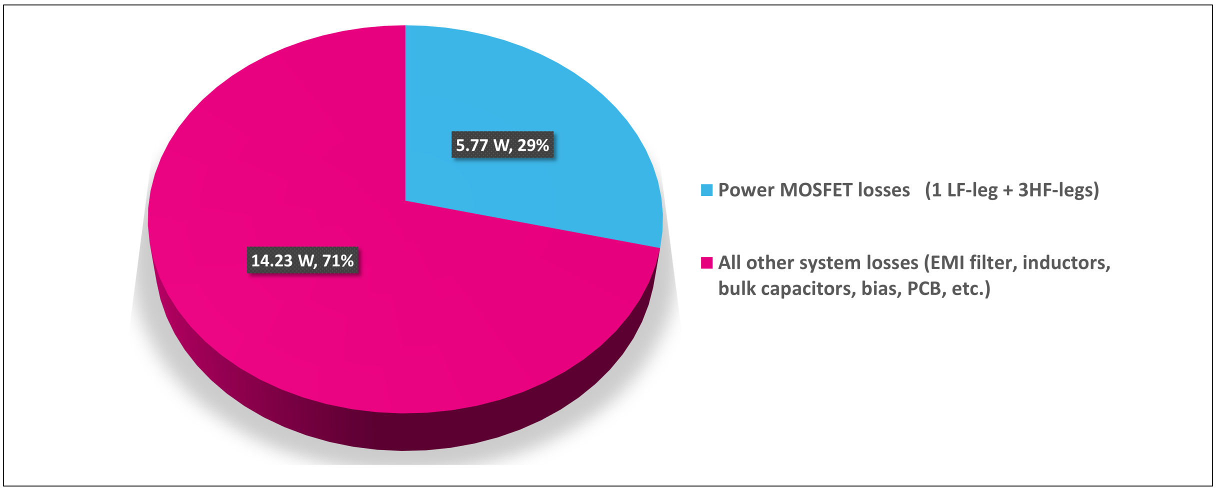

The previous equations can be used by a minimum power losses-based algorithm, so it is possible to automatically find the best device, from ST portfolio, starting only by PFC specifications.

It is necessary to observe that the previous formulas give only an estimation of the losses, therefore the actual losses will be verified only by experimental results.

4 eDesignSuite online design tool

eDesignSuite is a software tool developed by STMicroelectronics to help customers with several ST product configurations in power conversion applications.

4.1 ZVS-PFC step-by-step customization

Considering the STEVAL-TTPPFC01 as reference design, it is possible to customize a totem pole ZVS-PFC for a specific application [6]. Figure 7 shows the workspace for the selected customization, containing the general info (main specs, converter topology, BOM, Bode stability plots, etc.)

Figure 7. eDesignSuite ZVS-PFC main page

By clicking on [**CHANGE SPECIFICATIONS**], it is possible to access to the project wizard and customize the different circuit sections, including I/O stage, boost inductor, switch selections, sensing design, etc, as shown in the following figure.

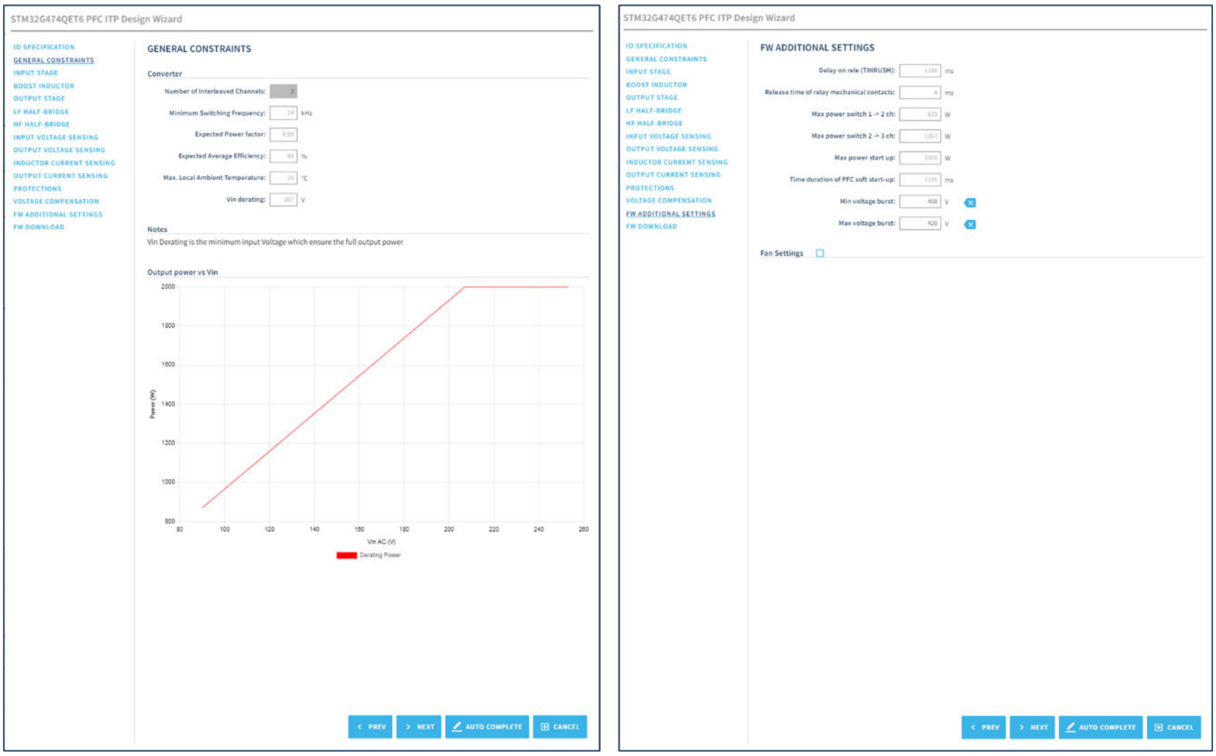

Figure 8. eDesignSuite ZVS-PFC step-by-step customization

4.2 Firmware download

After a few clicks the STM32CubeMX (.ioc) configuration file and the customized firmware pack can be downloaded as illustrated in Figure 9.

The generated code supports the following IDE tools:

- STM32CubeIDE
- IAR Embedded Workbench
- Keil uVision5

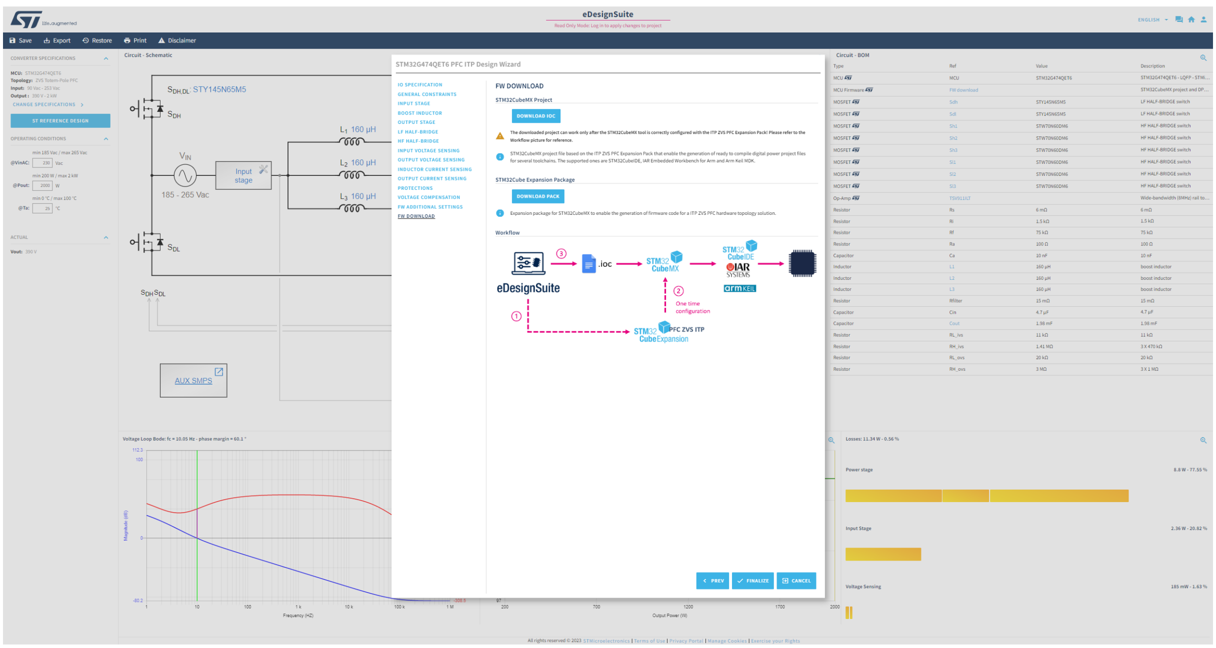

Figure 9. eDesign ZVS-PFC firmware download

It is recommended to use the following optimization options for compiling the downloaded firmware:

- STM32CubeIDE → **optimize for speed (- Ofast)**
- IAR Embedded Workbench → **high speed**
- Keil uVision5 → **Level 3 (-O3)**

5 Experimental results

Following connection to the grid, the auxiliary power supply starts, and the STM32G474QE together with all analog circuitry is supplied. **During the output capacitor precharging phase, the board must be in no-load condition** and the inrush current is limited by an input series resistor that is shorted by a relay at the end of this phase. If the grid parameters (voltage and frequency) are within the allowed range, the no-load startup bounds the output voltage between 400 V and 426 V (with burst mode operation, Figure 11), while the **load startup is admitted only after the relay is closed** and the nominal output voltage of 390 Vdc is reached after a soft ramp (see Figure 12).

Once the startup phase has finished, a green LED indicates that the PFC output has reached the setpoint value.

Figure 10. No-Load startup

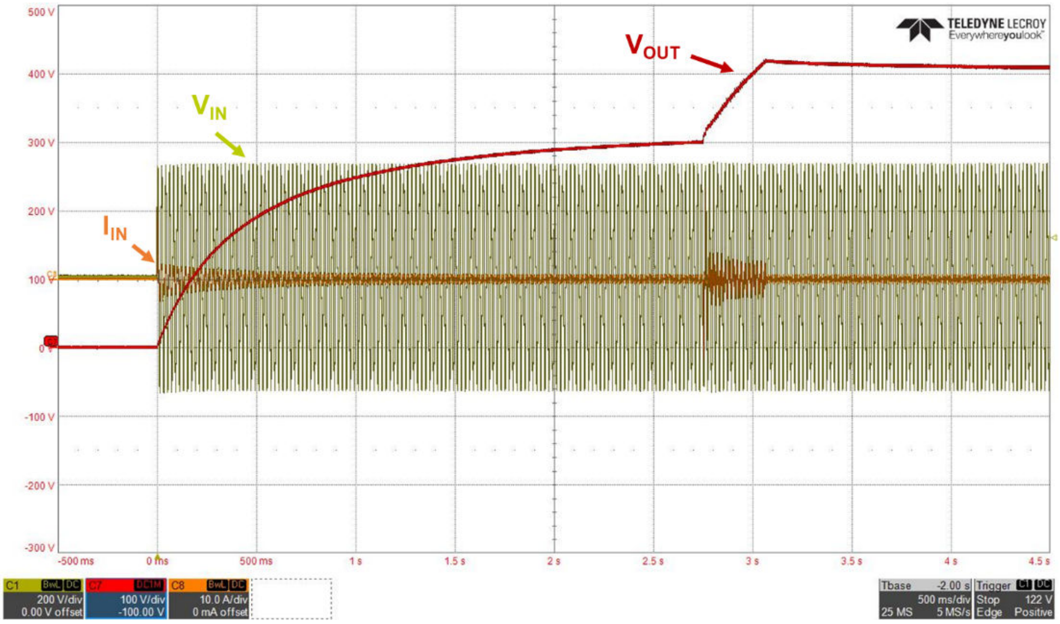

Figure 11. Burst mode operation

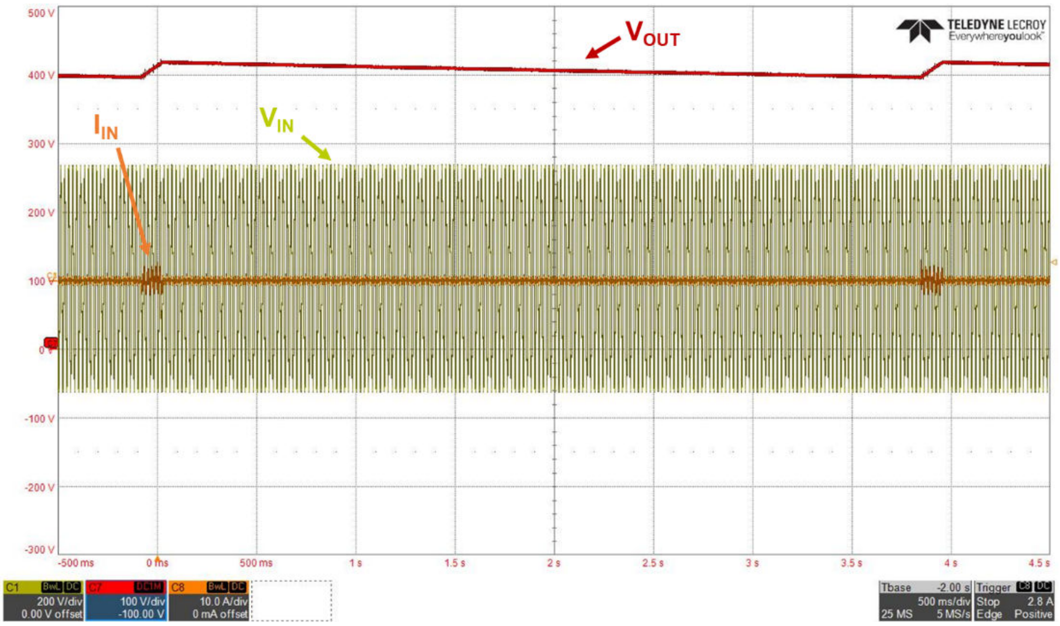

Figure 12. **Load startup in case of an autorecovery after a wait/error condition (input undervoltage)**

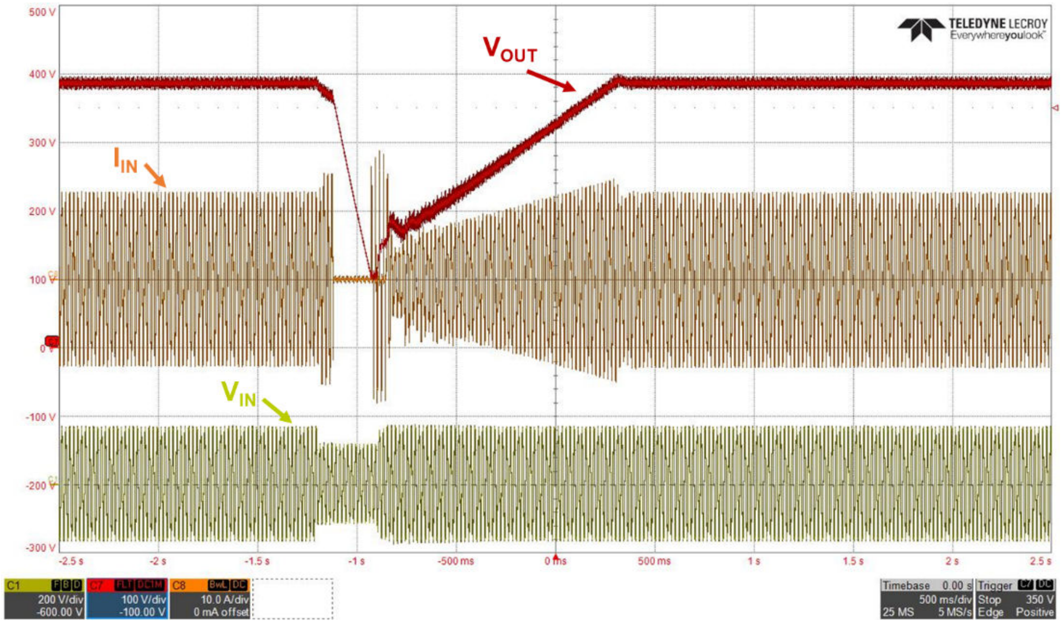

Figure 13 shows the inductor currents waveforms of the converter. The interleaving operation is evident in both two-channel and three-channel configuration.

Figure 13. **Interleaved inductor currents**

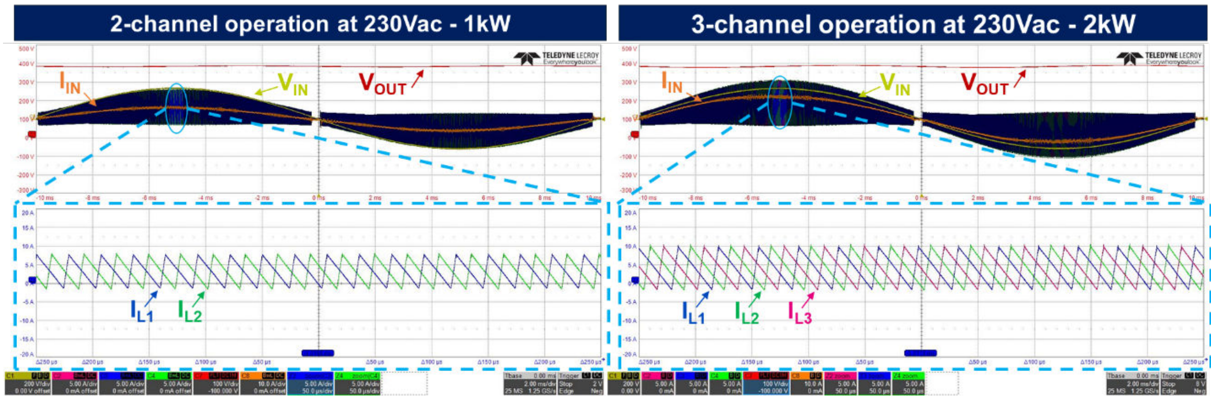

The correct behavior of the ZVS operation is shown in Figure 14, at the peak of the input voltage for both positive and negative resonance transitions.

Figure 14. **ZVS waveforms of one channel at 230 Vac and full load**

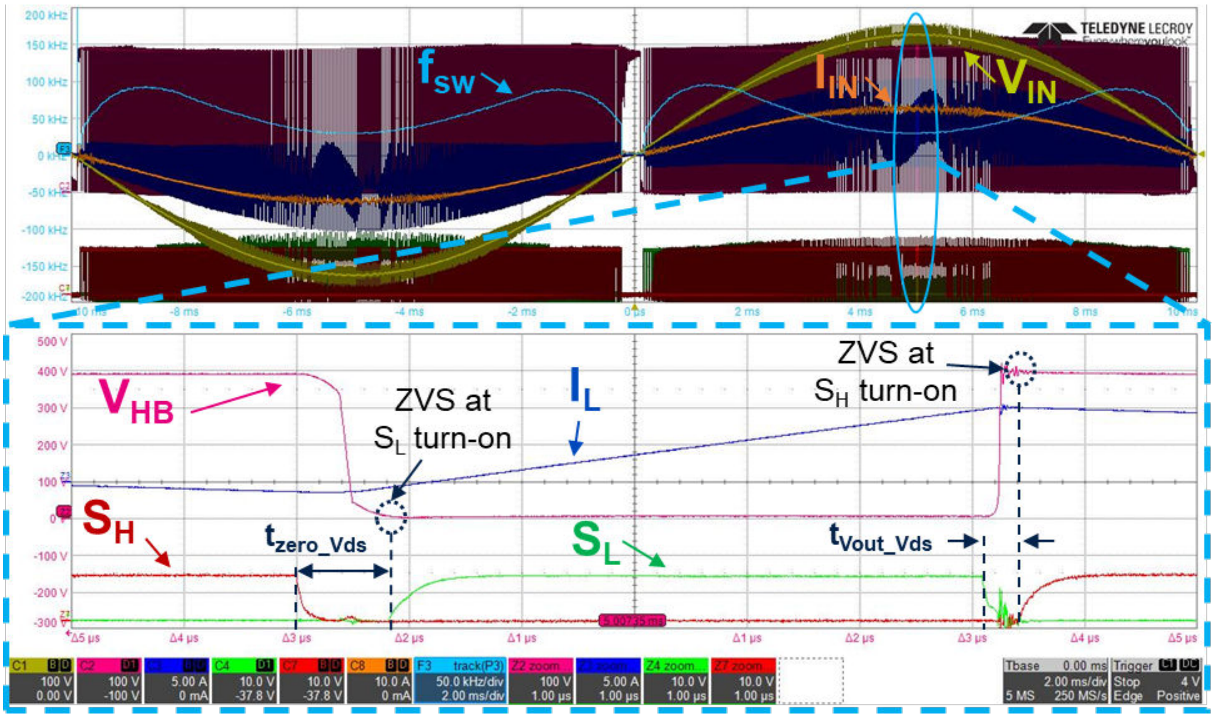

The steady-state operation of the STEVAL-TTPPFC01 is shown in Figure 15 and Figure 16 for low and high-line operation respectively. The input current is sinusoidal shaped and in phase with input voltage, as desired, while the output voltage is kept constant at the setpoint level of 390 V, confirming the correct PFC operation.

Figure 15. **Steady-state waveforms at 115 Vac and 1 kW load**

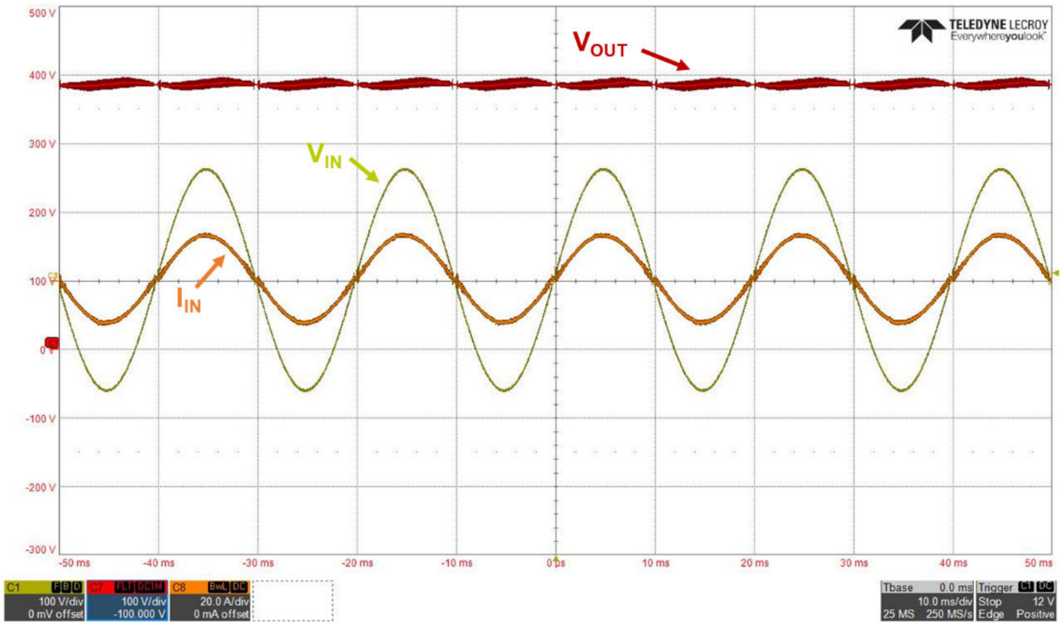

Figure 16. **Steady-state waveforms at 230 Vac and 2 kW load**

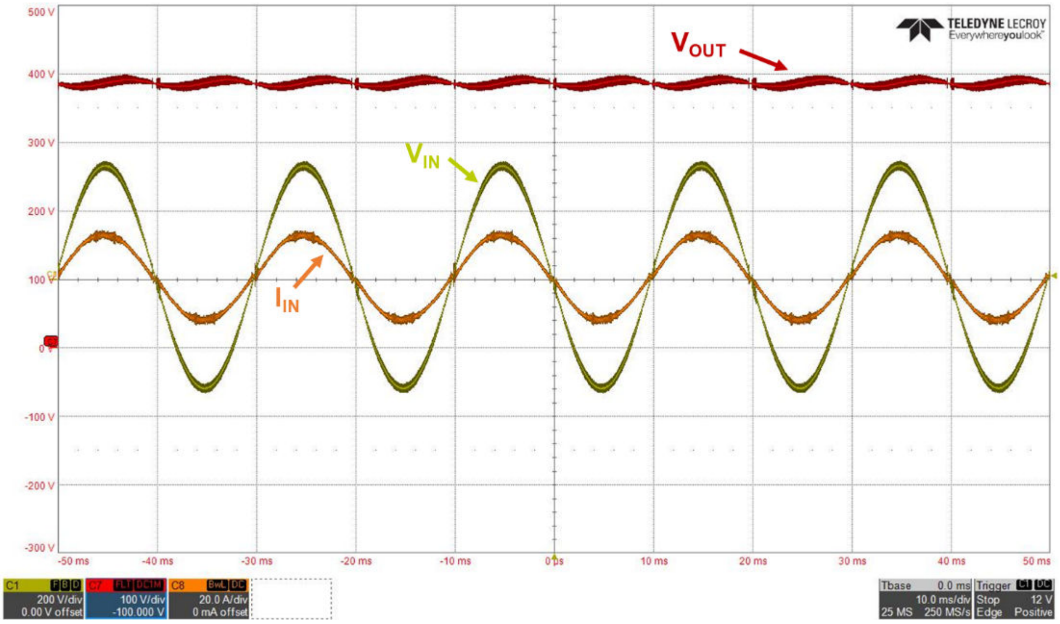

Figure 17. **Load step transition, 10% - 100% -10%, at 230 Vac**

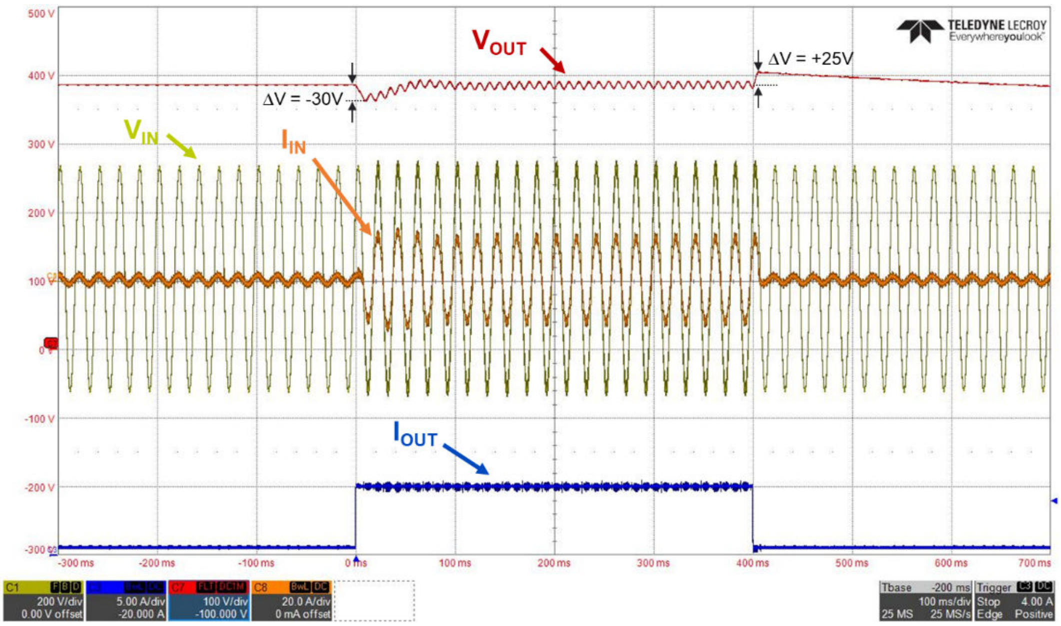

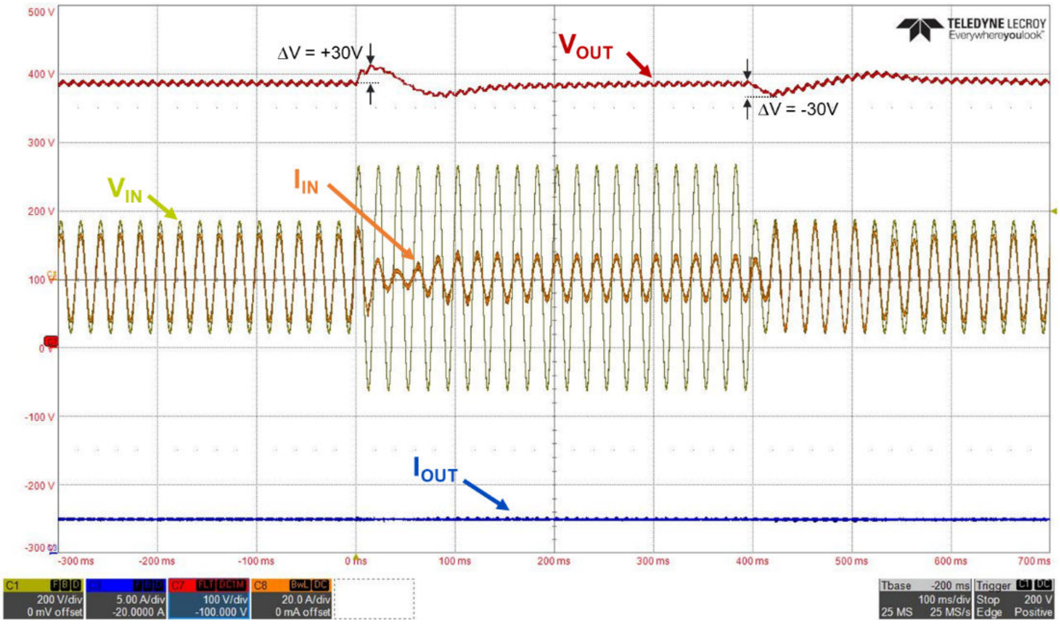

Figure 18. **Vin step transition 115-230 Vac at 1 kW load**

The transient behavior of the PFC is tested under load/input step transitions, represented in Figure 17 and Figure 18. For both the cases a fast dynamic response is obtained, thanks to the input and load feedforwards, and the dc bus voltage is tightly regulated at the reference value.

The line drop-out test is highlighted in Figure 18 in the worst case, occurring when the input voltage returns to its peak value. The hold-up requirement is met, and the reliability of the hysteresis current control is confirmed.

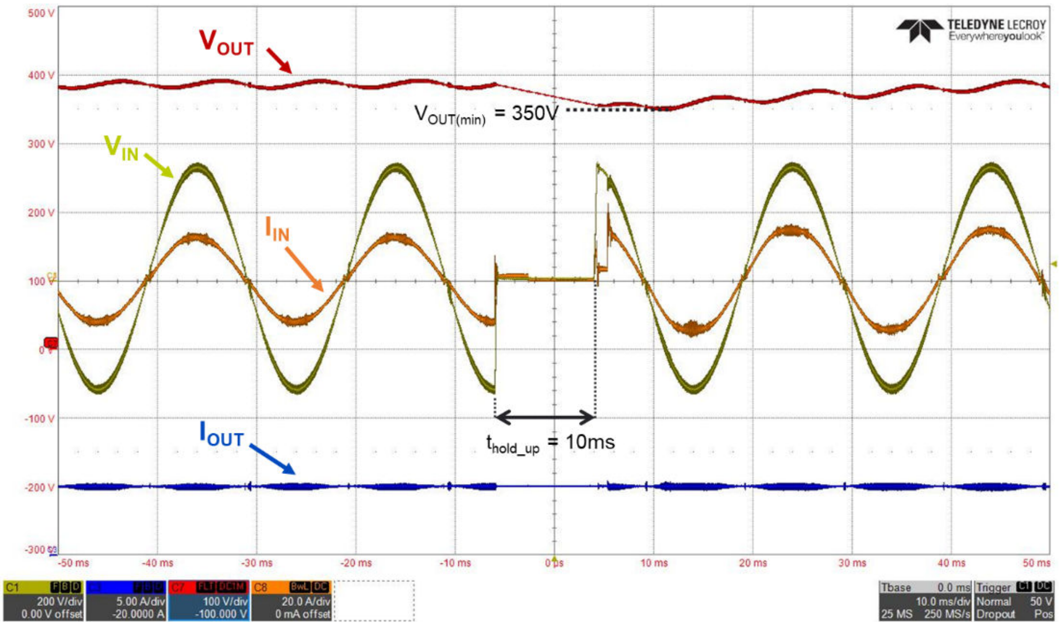

Figure 19. **Line drop-out test at 230 Vac and 2 kW load**

A precision power analyzer (Yokogawa WT1804E) was used to measure the total efficiency (also including the auxiliary power supply), power factor (PF) and the total harmonic distortion of the input current (THDi), according to the measurement setup of Figure 20.

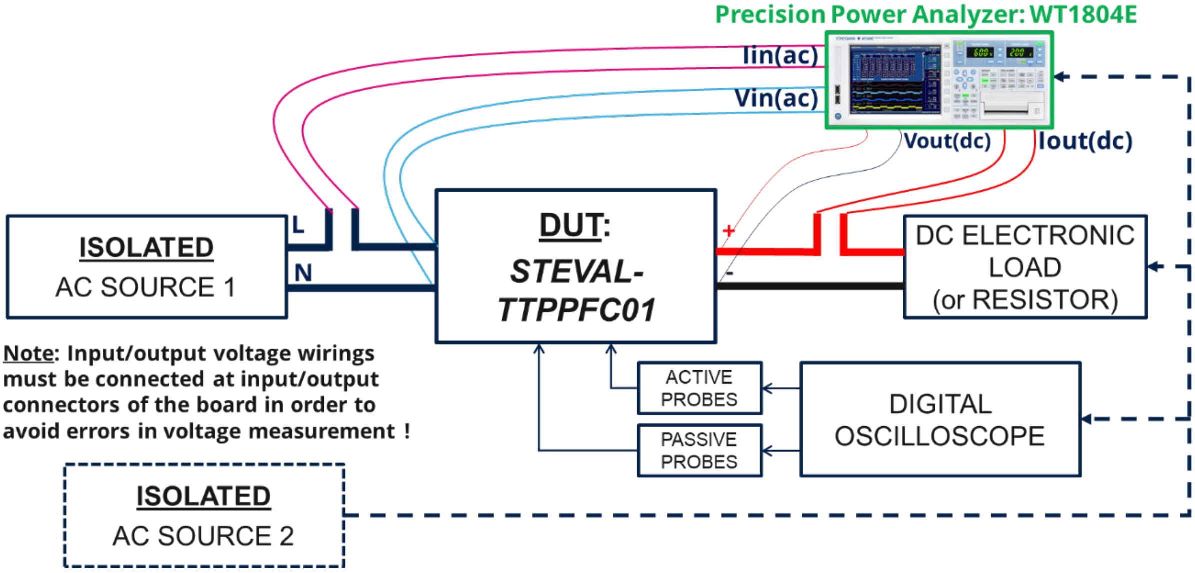

Figure 20. Measurement setup of the STEVAL-TTPPFC01.

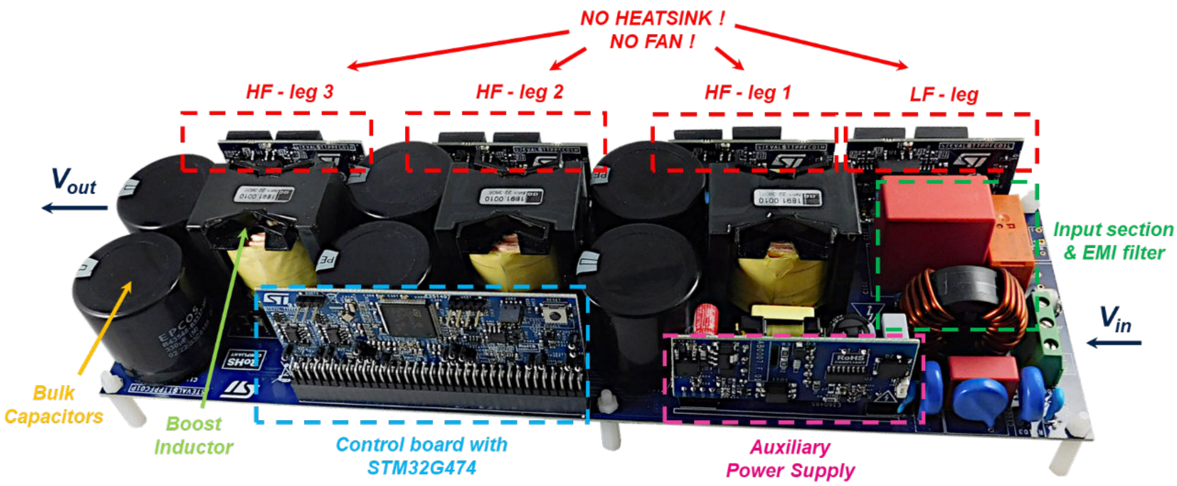

Figure 21. Main sections and modules of the STEVAL-TTPPFC01.

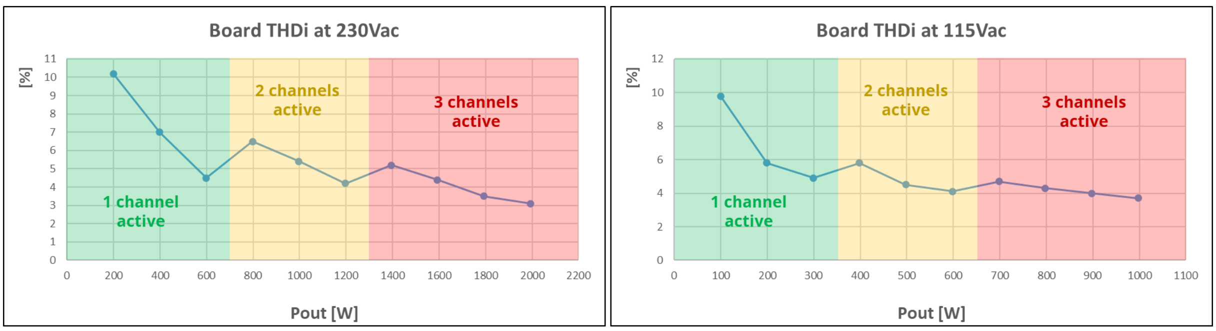

Figure 22. Input current THDi [%] vs output power.

Figure 23. **PFC power factor vs output power.**

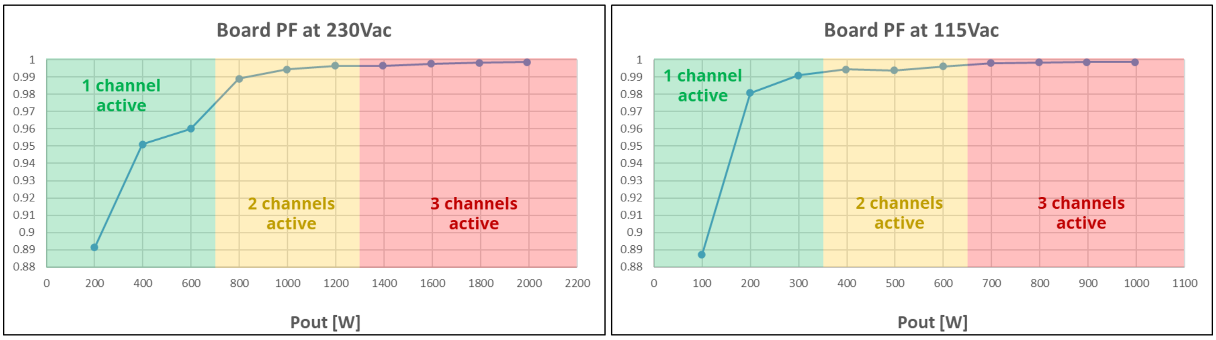

The input current THDi (see Figure 21) is below 10% for a load higher than 10%. It decreases down to 3% at 230 Vac (full load) and below 4% at 115 Vac (1 kW load). An almost unity power factor is achieved, in Figure 22, with values higher than 0.99 for load higher than 15% and 40% of rated power, at 115 Vac and 230 Vac respectively.

Thanks to the combination of bridgeless topology, ZVS operation, and phase shedding control strategy, the measured efficiency results in an extremely high and flat curve **≥99.2% for load higher than 50%** at 230 Vac (peak of 99.3% at 1200 W). This result is suitable for meeting the most stringent requirements of new standards and regulations.

Also, at 115 Vac, the STEVAL-TTPPFC01 delivers a very high efficiency >98% for loads higher than 20%, with a maximum of 98.55% at 1 kW. In this case, the typical higher conduction losses (compared to 230 Vac) are partially compensated by a lower average switching frequency (see Figure 26), which helps to reduce the overall system losses, including MOSFET and passives. **For both high and low line measurements, the bias and all other losses are included since the board is self-supplied by the integrated AUX module**.

Figure 24. **PFC efficiency vs output power at 230 Vac.**

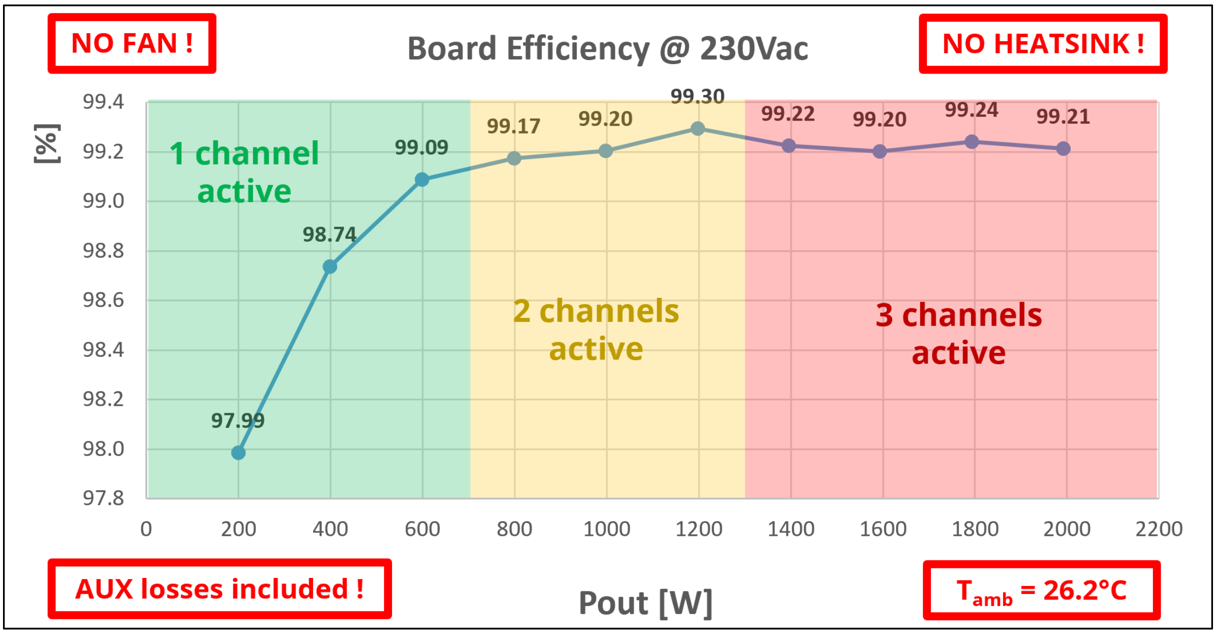

Figure 25. **PFC efficiency vs output power at 115 Vac.**

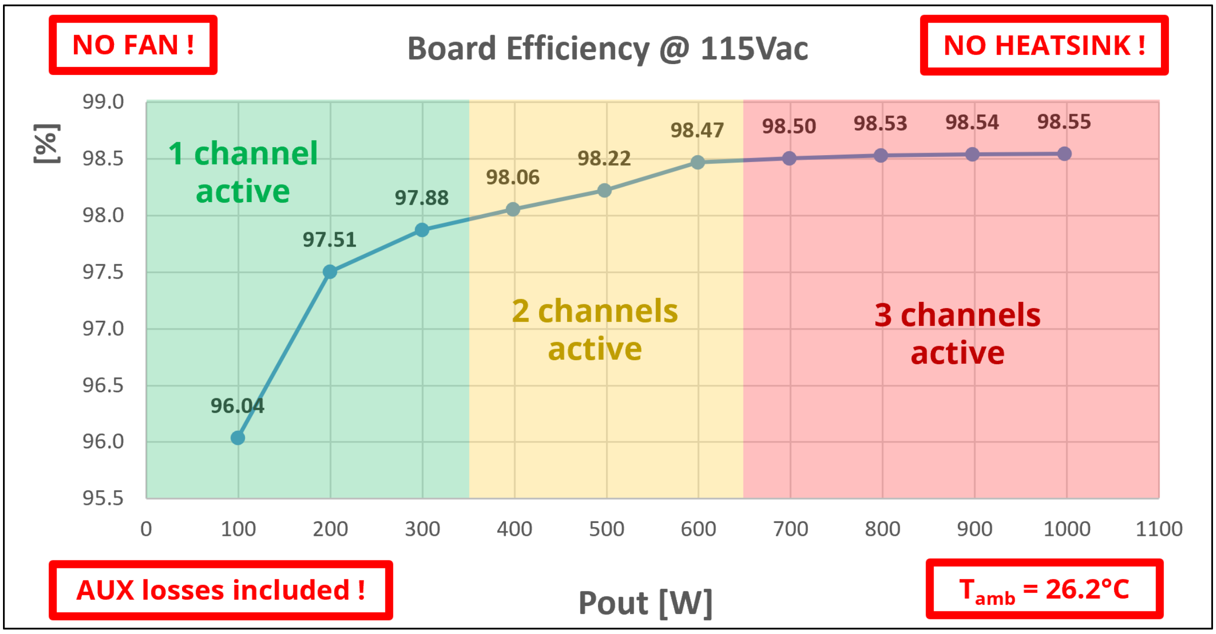

Figure 26. **Average switching frequency behavior for each channel vs output power.**

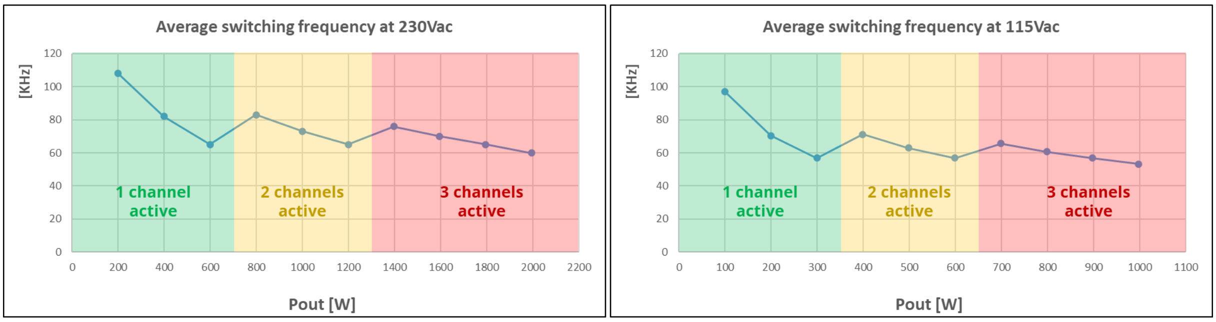

To confirm the previous measurements, a thermal analysis of the power devices was done at 230 Vac and full load (see Figure 27), obtaining the results reported in Table 2. From a thermal point of view the power dissipated in each MOSFET can be calculated considering its temperature, the ambient temperature, and the thermal resistance of the package:

$$P_{single\_LF\_th} = \frac{T_{LF\_MOSFET} - T_{amb}}{R_{thj-amb\_LF}} = \frac{48 - 26.2}{30} = 0.727W \tag{28}$$

$$P_{single\_HF\_th} = \frac{T_{HF\_MOSFET} - T_{amb}}{R_{thj-amb\_HF}} = \frac{47.9 - 26.2}{50} = 0.434W \tag{29}$$

For both LF-leg and HF-legs, the results are reported in the last column of Table 2.

The LF-leg includes only conduction losses, so no further details are needed as the result of thermal equation (28) is perfectly aligned with theoretical equation (24). Instead, to obtain the losses distribution in the HF-leg, the three loss components (conduction, switch-off, and driving) must be derived. The following considerations are here done:

1. The driving loss does not significantly affect the heating of the MOSFET, so it can be excluded from the thermal calculation, but it is counted in the AUX power supply losses by equation (20). Thus, the results of equations (28) and (29) are attributed to the conduction and switch-off losses only.
2. It's very difficult to estimate the switch-off losses because of the uncertainty in the estimation of the t_{fall} of the MOSFET in a PFC, where the operating point continuously changes along the sinusoidal input voltage.

Consequently, the preferred approach here is to evaluate first the conduction losses using the measured data of Table 2 in equation (22). Then, calculate the switch-off losses as the difference between the thermal losses and conduction losses:

$$P_{cond\_HF\_th} = 1.23 \cdot 0.036 \cdot 2.72^2 = 0.327W \quad (30)$$

$$P_{off\_HF\_th} = P_{single\_HF\_th} - P_{cond\_HF\_th} = 0.434 - 0.327 = 0.106W \quad (31)$$

The rms current of the HF-MOSFET reported in Table 2 is measured over the whole mains period so conduction losses obtained in equation (30) do not need to be divided by 2 as in equation (25), the same consideration is valid for the result of equation (31).

Finally, it should be noted that the thermal result in (31) is much lower than theoretical value in equation (26), confirming the real difficulty in the switch-off losses estimation.

Figure 27. **MOSFET temperatures at 230 Vac and 2 kW load.**

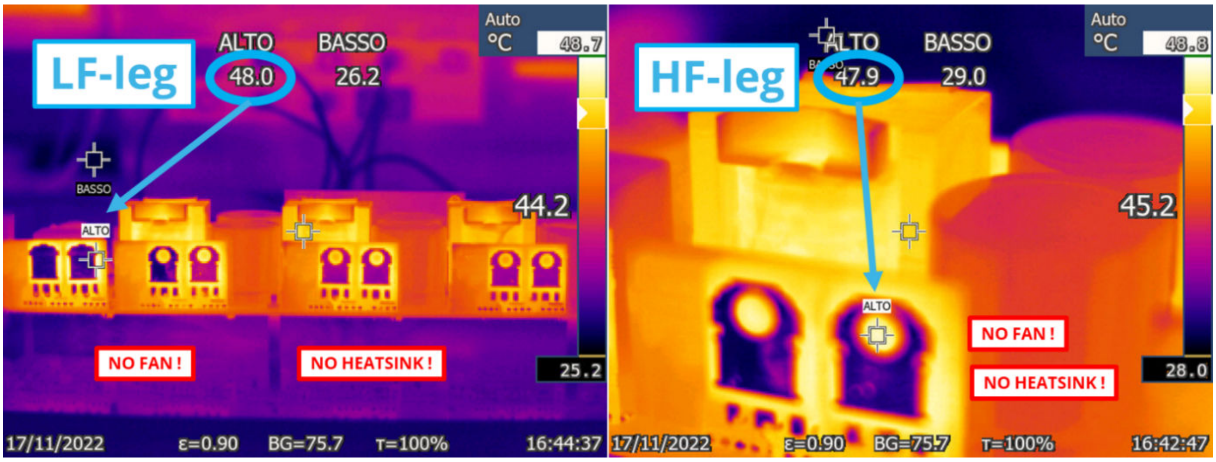

Table 2. **Measurements and data for thermal analysis at 230 Vac and 2 kW load**

MOSFET PNs	Device measurement						
	fsw(avg) [kHz]	Isw(rms) [A]	Temp. Coeff. [°C]	TMOSFET [°C]	Tamb [°C]	Rthj-amb [°C/W]	Losses [W]
STW70N60DM6 (HF-leg)	60	2.72	1.23	47.9	26.2	50	0.434
STY145N65M5 (LF-leg)	-	-	1.23	48	26.2	30	0.727

Figure 28. Power MOSFETs total losses at 230 Vac and 2 kW load.

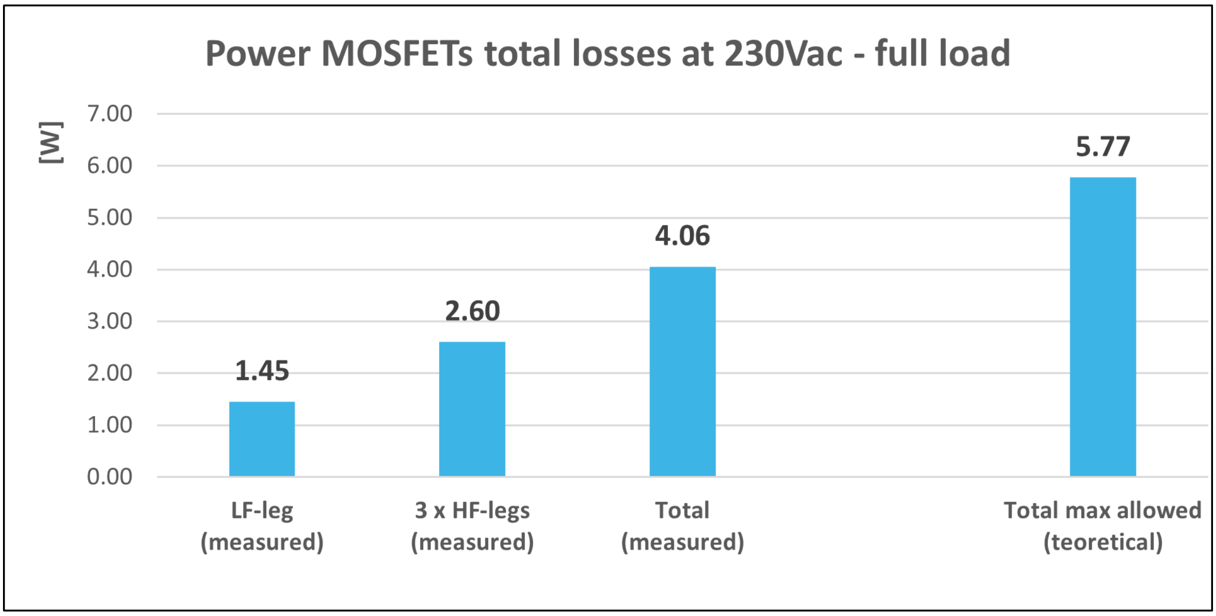

Figure 29. Detailed losses distribution in all the HF-legs at 230 Vac and 2 kW load.

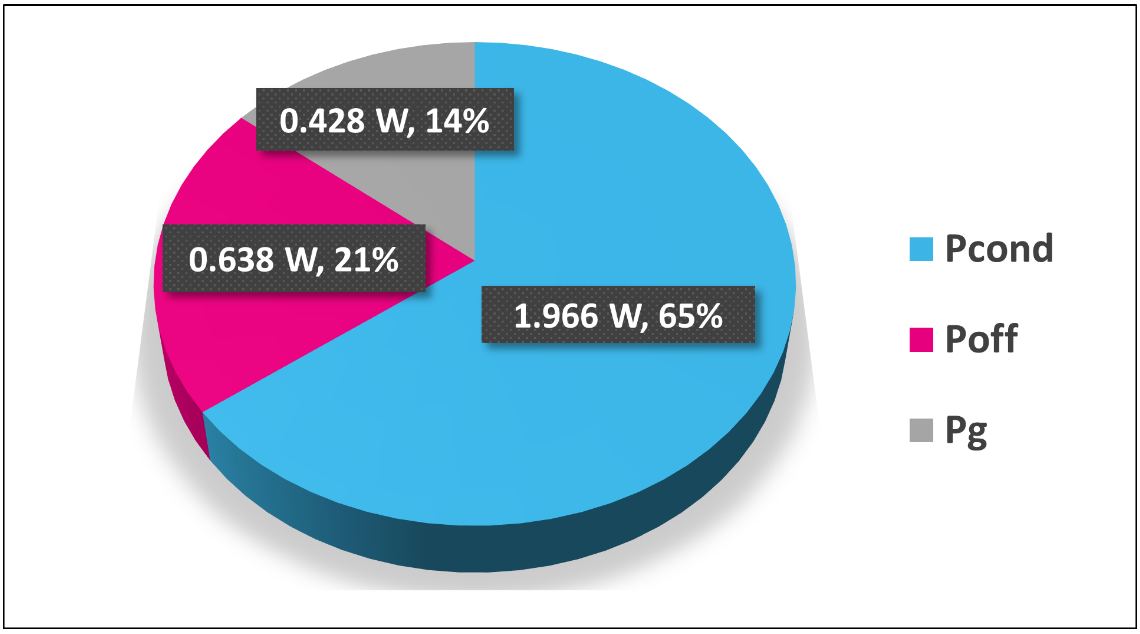

The total MOSFET losses measured with the thermal analysis are shown in Figure 28, including one LF-leg and three HF-legs.

The initial target of 99% efficiency for the STEVAL-TTPPFC01 (see Figure 6) is fully achieved and even exceeded, since total losses of all the power MOSFETs are 4.06 W, so quite lower than the maximum allowed of 5.77 W. This last result is a further confirmation of the extremely high system efficiency of 99.21% obtained for the STEVAL-TTPPFC01 at nominal input voltage 230 Vac and full load.

6 EMI test results

The precompliance conducted EMI test for the CISPR 32, class A, have been performed with the connection scheme of Figure 30, the input filter of Figure 31, and the output filter of Figure 32.

A copper or aluminum plate with dimensions 20 x 40 cm can be used to realize the reference plane for ground return currents, imitating the chassis.

Figure 30. Connection scheme for EMI test of STEVAL-TTPPFC01

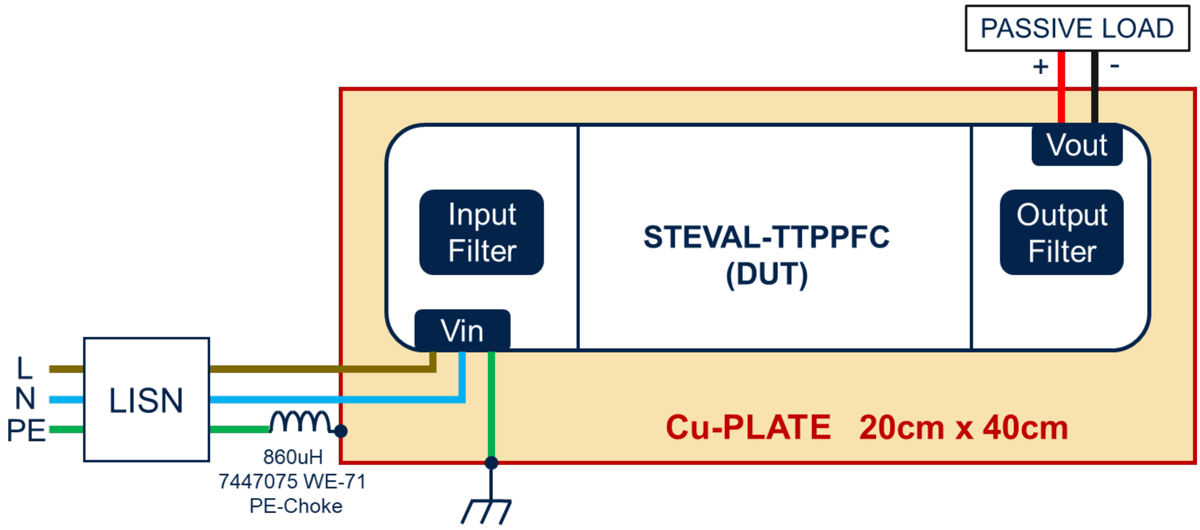

Figure 31. Input filter for EMI test of STEVAL-TTPPFC01

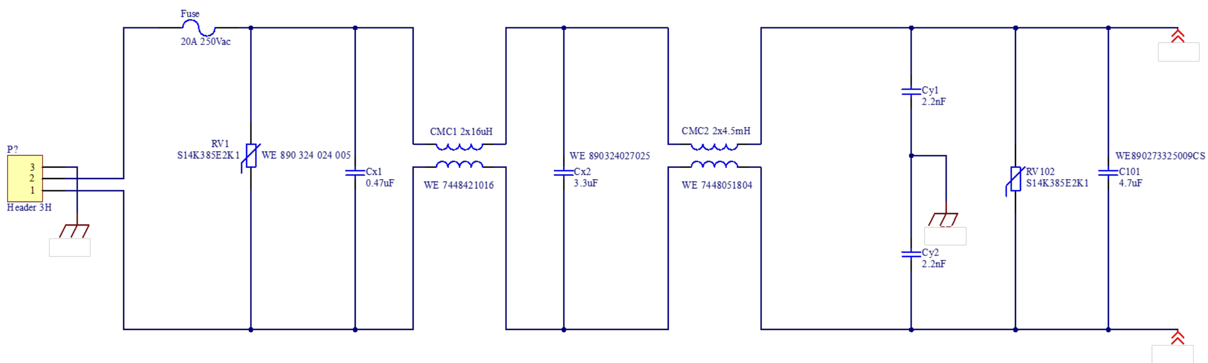

Figure 32. **Output filter for EMI test of STEVAL-TTPPFC01**

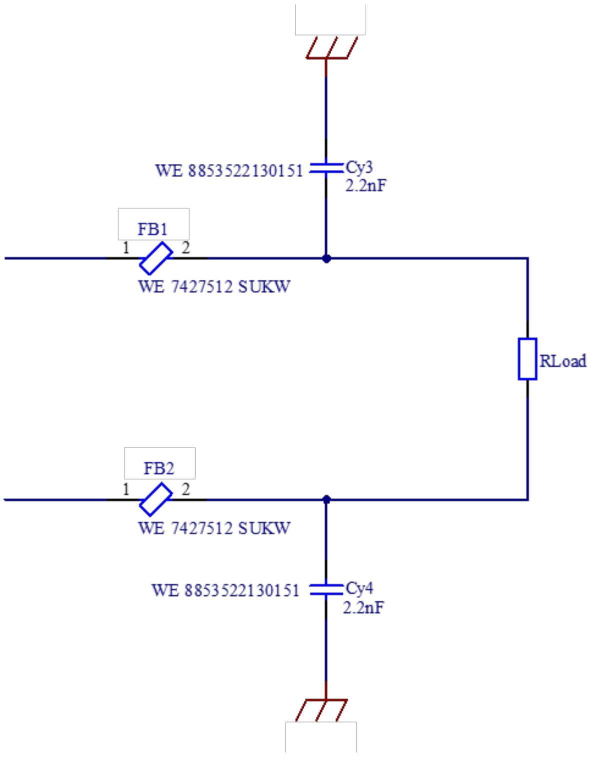

Figure 33. **Conducted EMI test result (pass) of STEVAL-TTPPFC01**

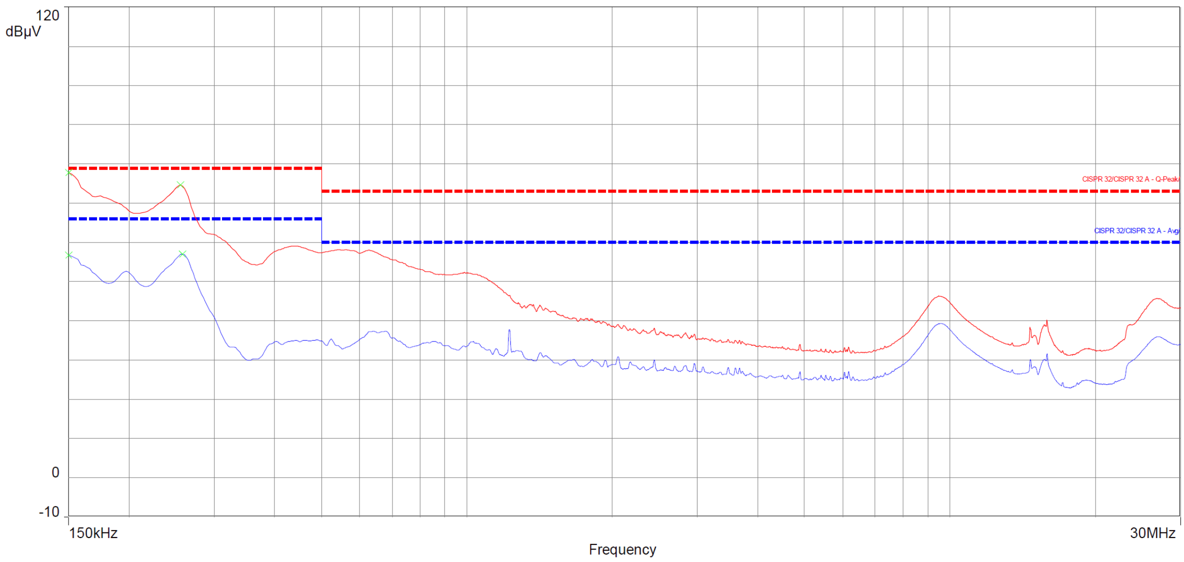

7 Schematic diagrams

Figure 34. STEVAL-TTPPFC01 - power board circuit schematic (1 of 5)

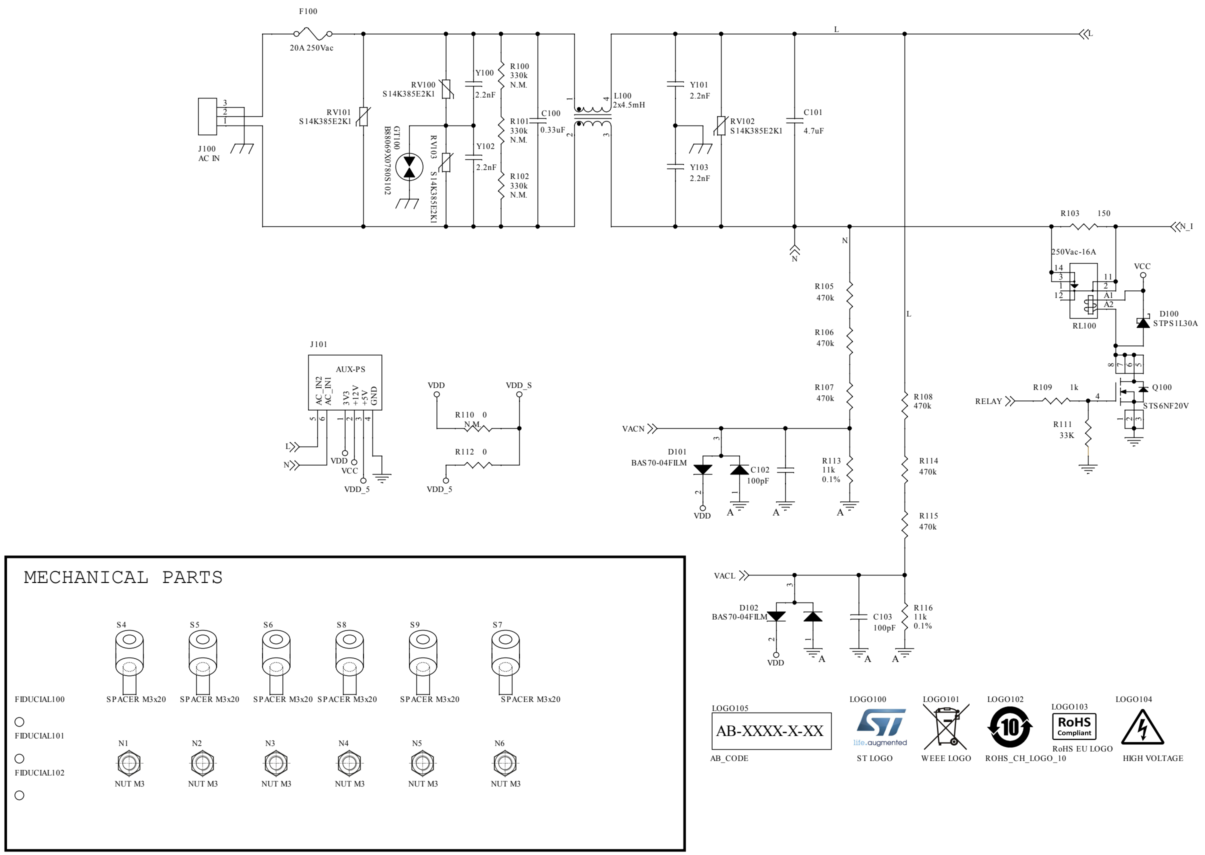

Figure 35. STEVAL-TTPPFC01 - power board circuit schematic (2 of 5)

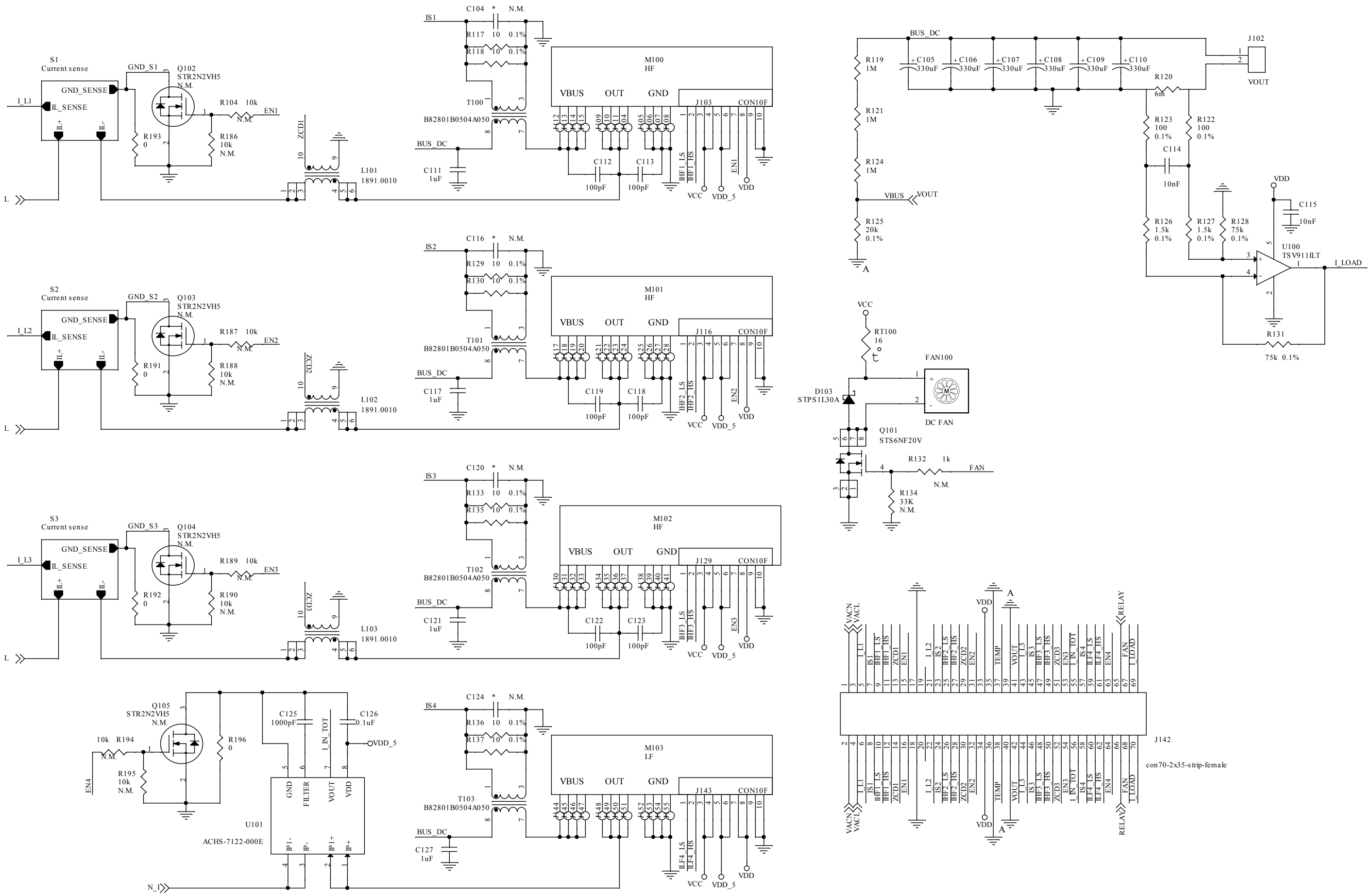

Figure 36. STEVAL-TTPPFC01 - power board circuit schematic (3 of 5)

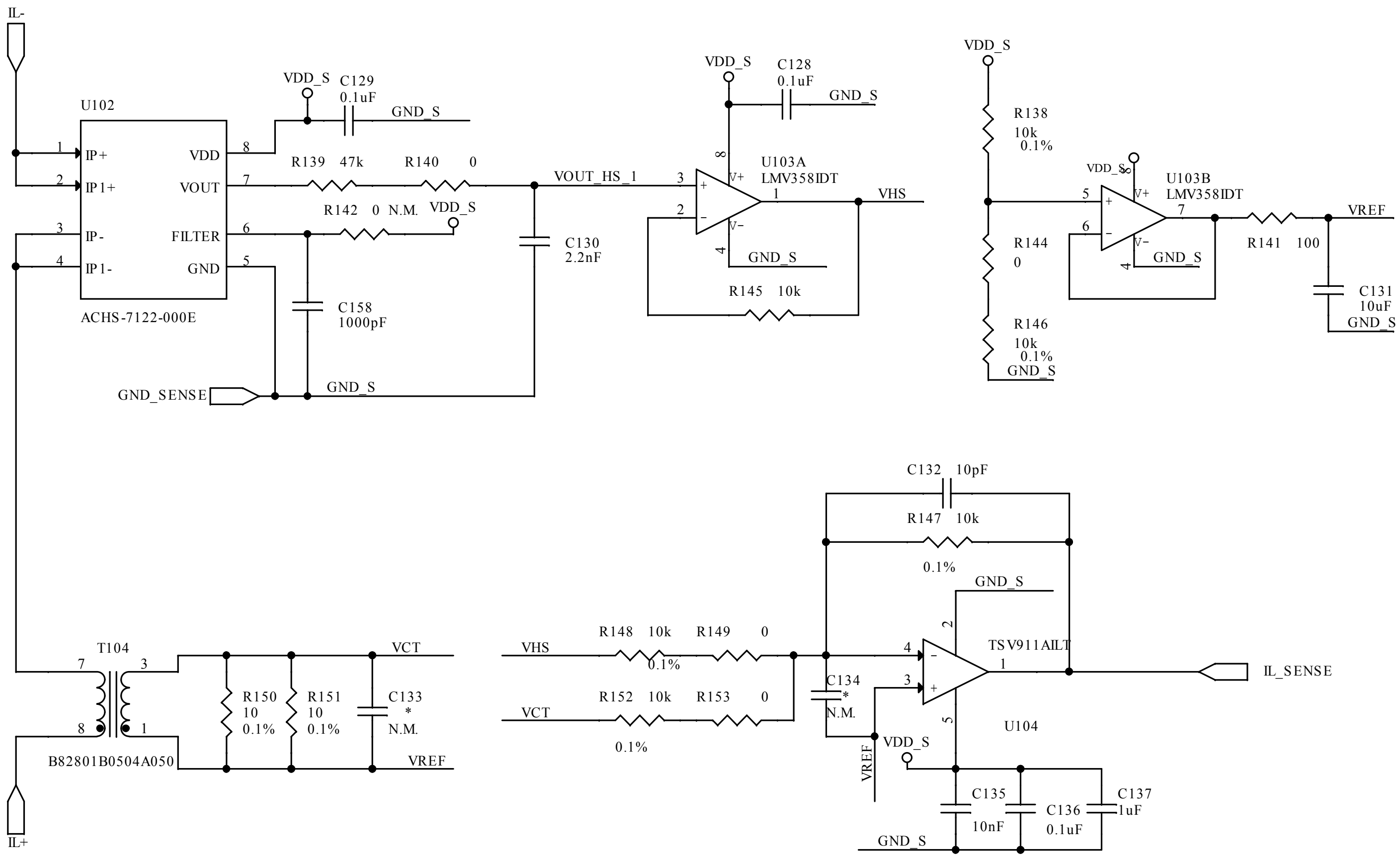

Figure 37. STEVAL-TTPPFC01 - power board circuit schematic (4 of 5)

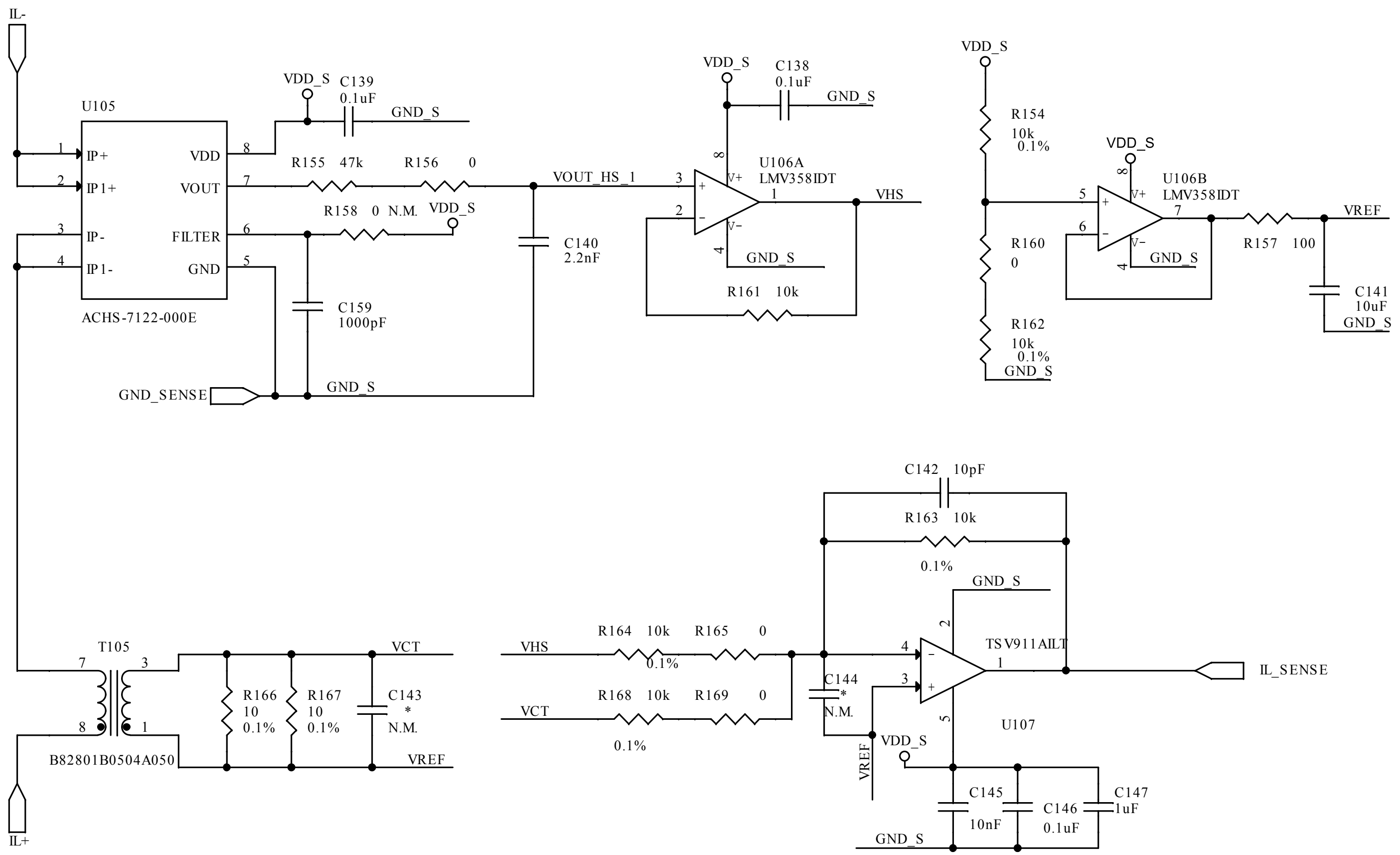

Figure 38. STEVAL-TTPPFC01 - power board circuit schematic (5 of 5)

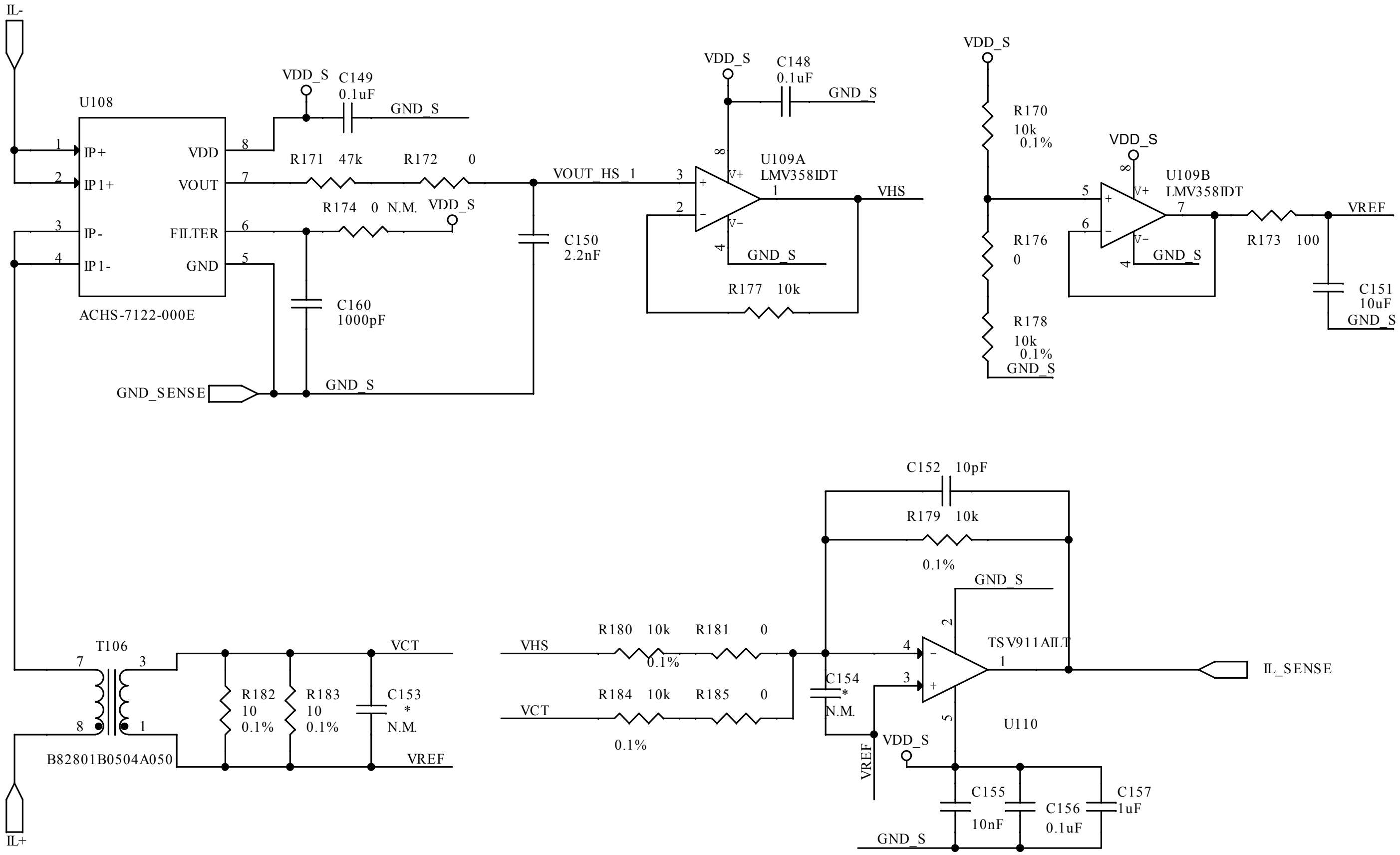

Figure 39. STEVAL-TTPPFC01 - control board circuit schematic (1 of 2)

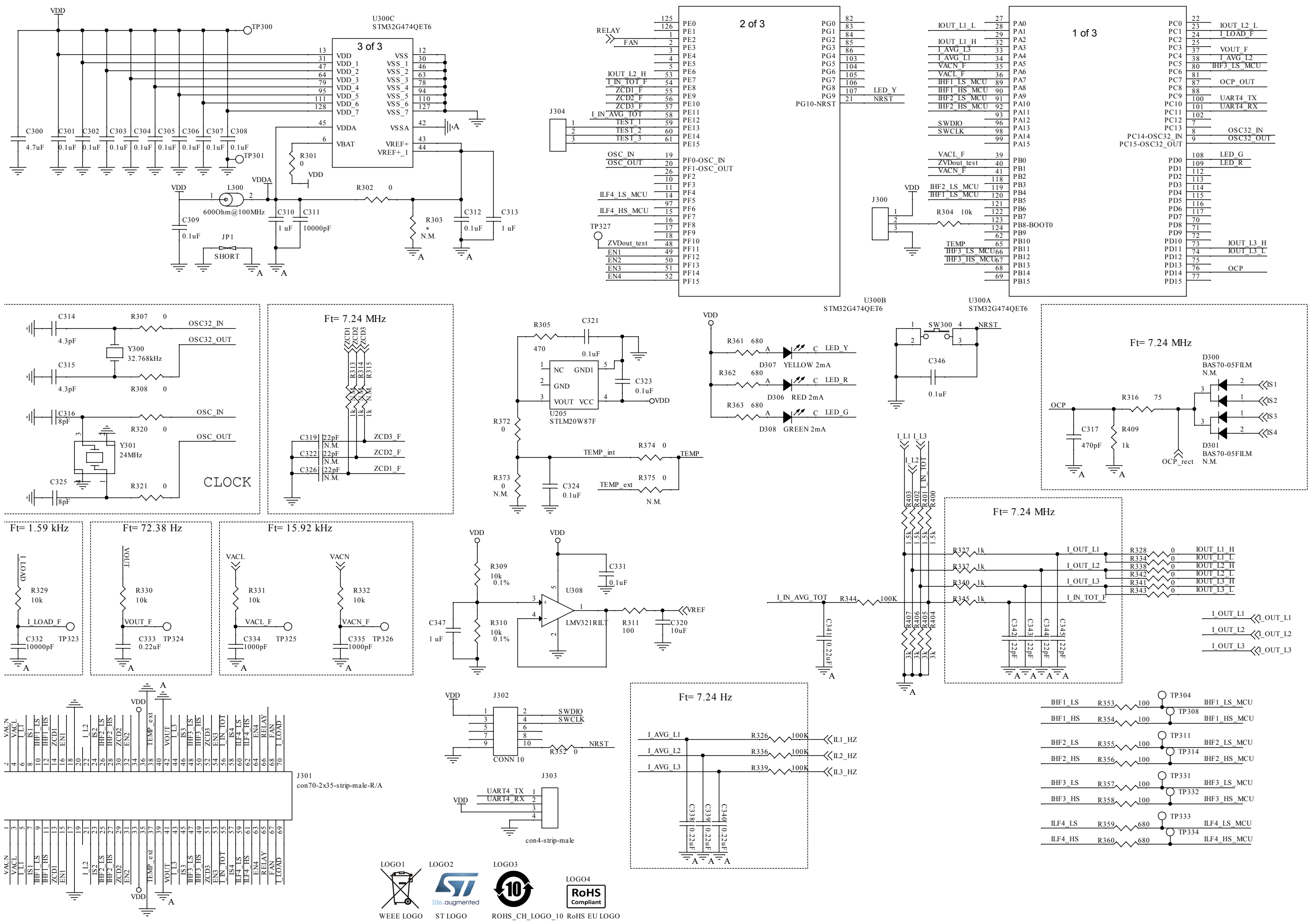

Figure 40. STEVAL-TTPPFC01 - control board circuit schematic (2 of 2)

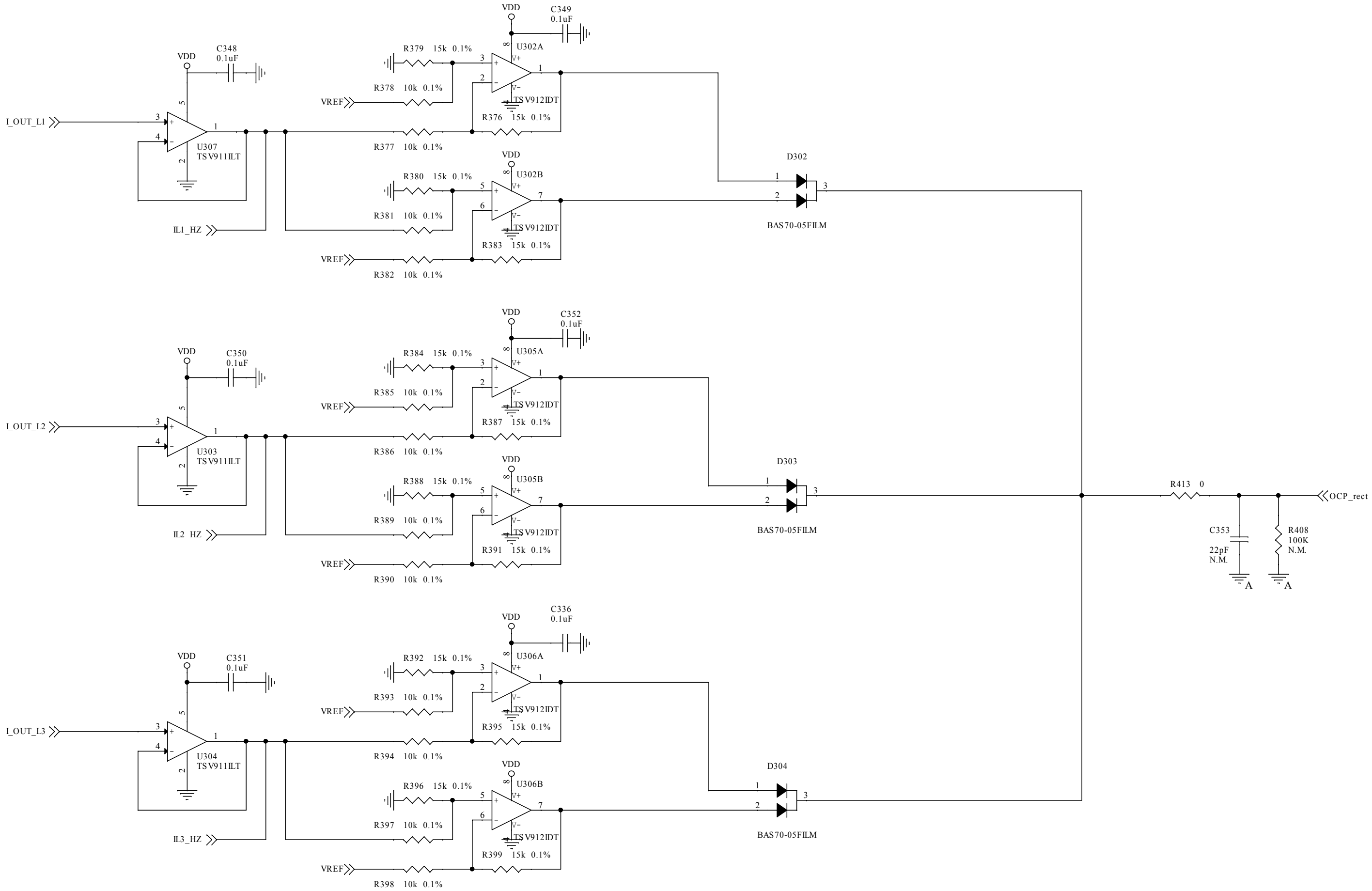

Figure 41. STEVAL-TTPPFC01 - auxiliary board circuit schematic

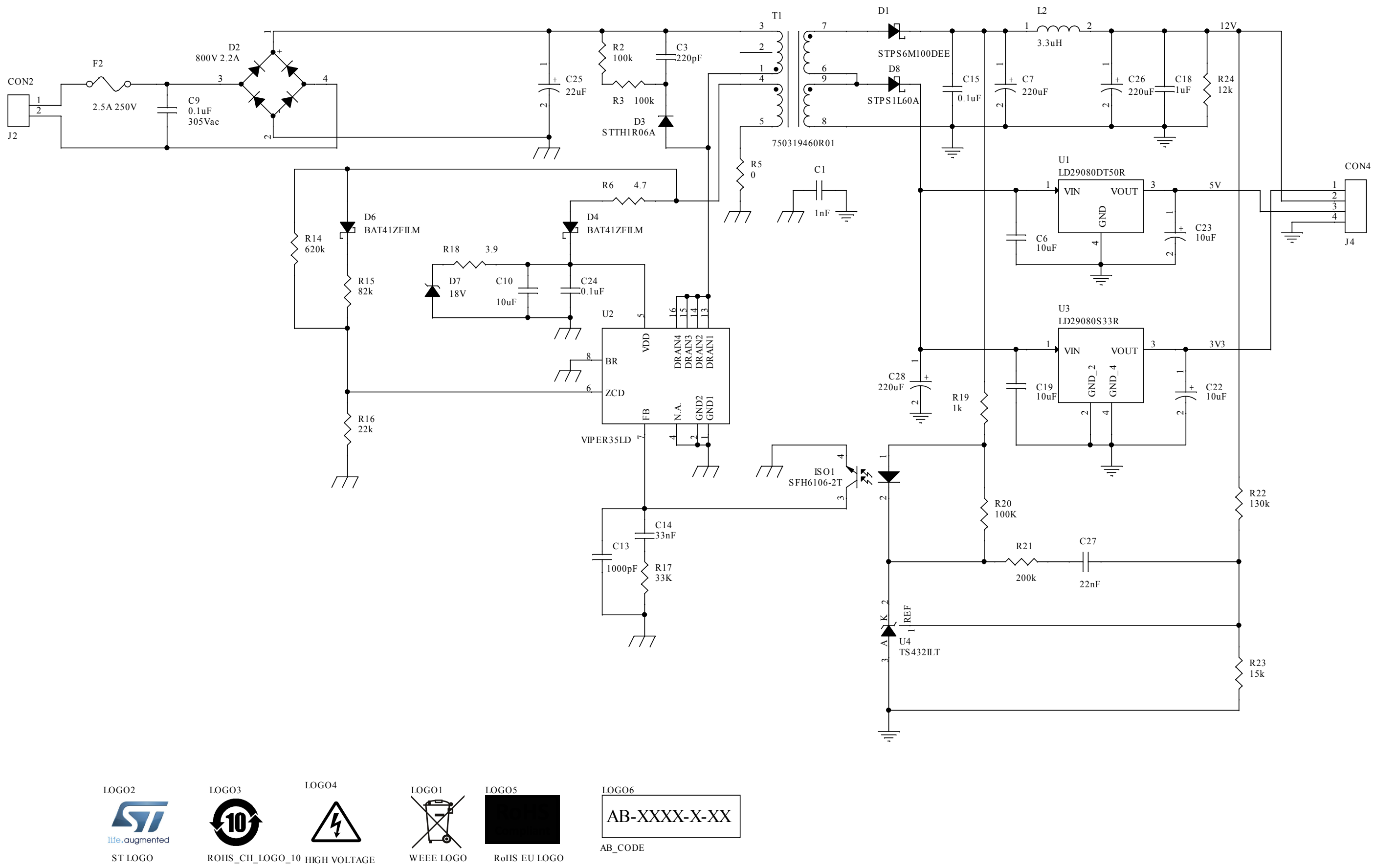

Figure 42. STEVAL-TTPPFC01 - high-frequency half-bridge board circuit schematic

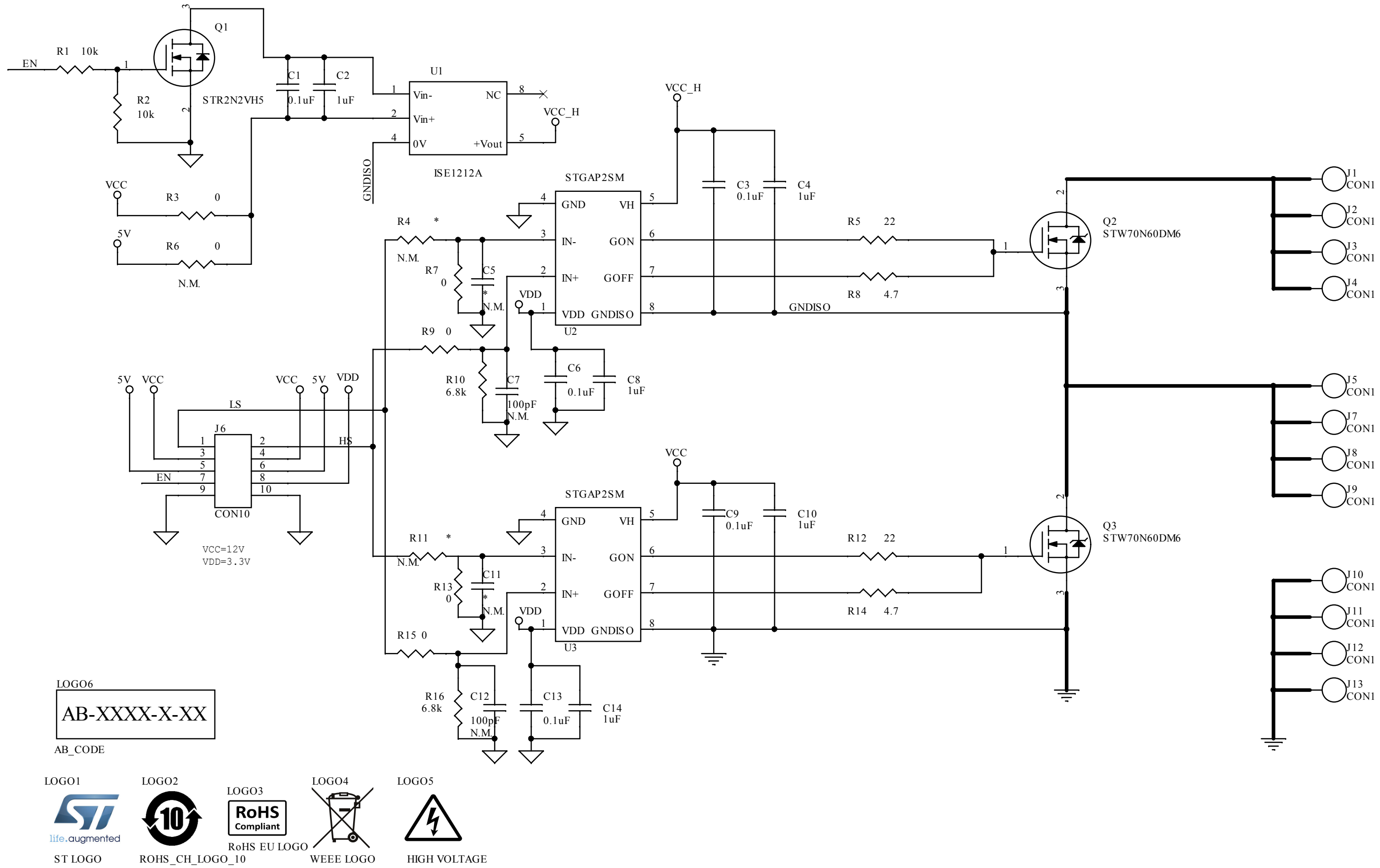

Figure 43. STEVAL-TTPPFC01 - low-frequency half-bridge board circuit schematic

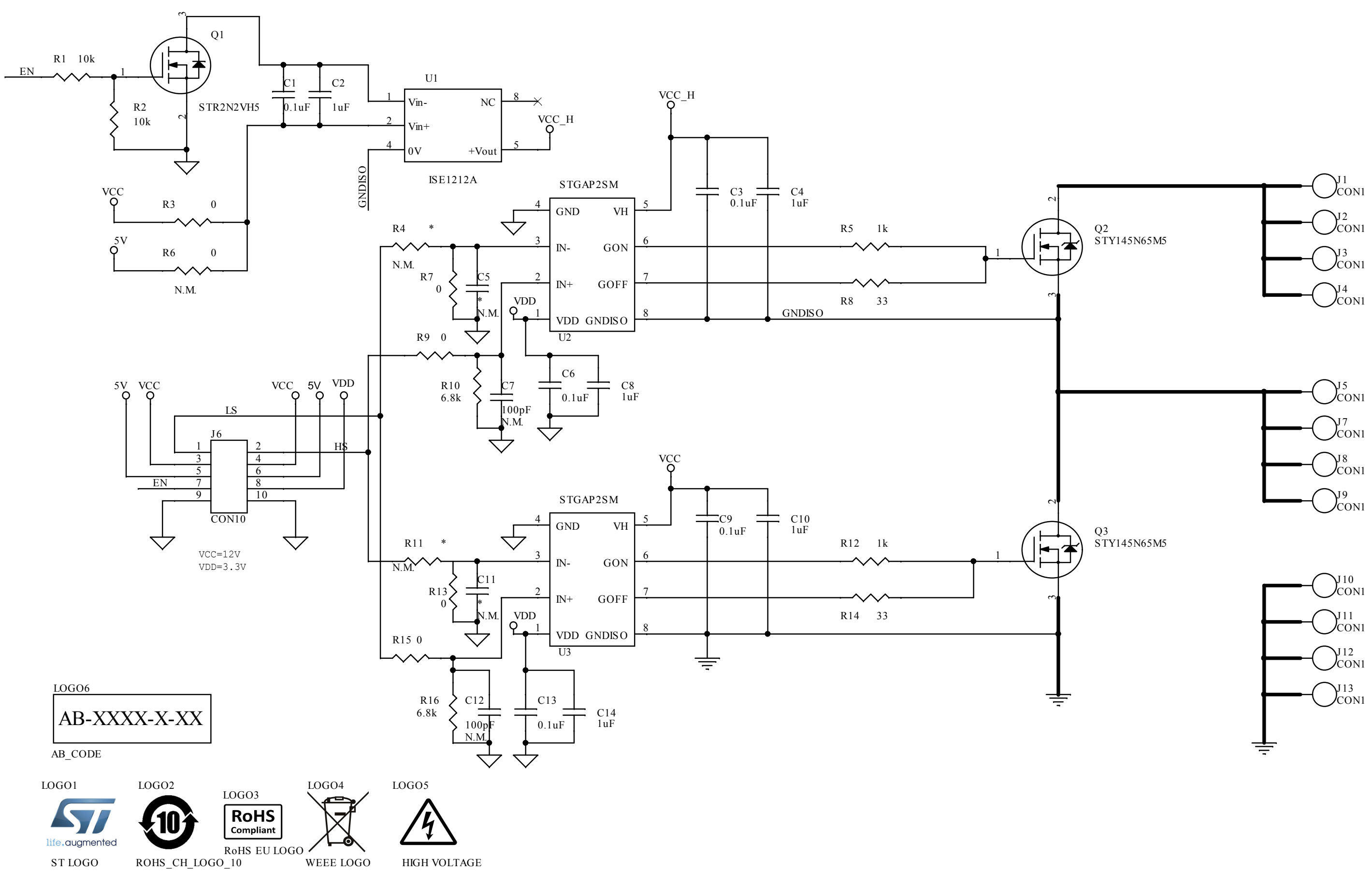

8 Bill of materials

Table 3. STEVAL-TTPPFC01 bill of materials

Item	Q.ty	Ref.	Part/Value	Description	Manufacturer	Order code
1	1	-	Table 4	Power board	ST	Not available for separate sale
2	1	-	Table 5	Control board	ST	Not available for separate sale
3	1	-	Table 6	Auxiliary board	ST	Not available for separate sale
4	3	-	Table 7	High-frequency Half-bridge board	ST	Not available for separate sale
5	1	-	Table 8	Low-frequency Half-bridge board	ST	Not available for separate sale

Table 4. Power board bill of materials

Item	Q.ty	Ref.	Part/Value	Description	Manufacturer	Order code
1	1	C100	0.33uF	CAP FILM 0.33UF 20% 305VAC RAD	EPCOS (TDK)	B32922C3334M000
2	1	C101	4.7uF	CAP FILM 4.7UF 20% 630VDC RADIAL	EPCOS - TDK Electronics	B32924H3475M
3	2	C102 C103	100pF	CAP CER 100PF 50V C0G/NP0 0603	Würth Elektronik	885012006057
4	10	C104 C116 C120 C124 C133 C134 C143 C144 C153 C154	*	CAPACITOR CERAMIC SMD 0603		
5	6	C105 C106 C107 C108 C109 C110	330uF	CAP ALUM 330uF 20% 450V SNAP	EPCOS - TDK Electronics	B43548B5337M060
6	4	C111 C117 C121 C127	1uF	Film Capacitors FILM CAP MKP PFC 1.0F 10% 630Vdc LS 22.5mm	EPCOS / TDK	B32673P6105K289
7	6	C112 C113 C118 C119 C122 C123	100pF	CAP CER 100PF 630V C0G/NP0 1812	AVX Corporation	1812CA101JAT2A
8	5	C114 C115 C135 C145 C155	10nF	CAP CER 10000PF 25V X7R 0603	Würth Elektronik	885012206065
9	4	C125 C158 C159 C160	1000pF	CAP CER 1000PF 25V C0G/NP0 0603	Würth Elektronik	885012006044
10	10	C126 C128 C129 C136 C138 C139 C146 C148 C149 C156	0.1uF	CAP CER 0.1UF 25V X7R 0603	Würth Elektronik	885012206071
11	3	C130 C140 C150	2.2nF	CAP CER 2200PF 25V X7R 0603	Würth Elektronik	885012206061
12	3	C131 C141 C151	10uF	CAP CER 10UF 16V X5R 0805	Wurth Electronics Inc.	885012107014

Item	Q.ty	Ref.	Part/Value	Description	Manufacturer	Order code
13	3	C132 C142 C152	10pF	CAP CER 10PF 50V C0G/NP0 0603	Würth Elektronik	885012006051
14	3	C137 C147 C157	1uF	CAP CER 1UF 16V X7R 0603	Würth Elektronik	885012206052
15	1	D100	STPS1L30A, SMA	DIODE SCHOTTKY 30V 1A SMA	STMicroelectronics	STPS1L30A
16	2	D101 D102	BAS70-04FILM, SOT23	DIODE ARRAY SCHOTTKY 70V SOT23-3	STMicroelectronics	BAS70-04FILM
17	1	D103	STPS1L30A, SMA	DIODE SCHOTTKY 30V 1A SMA	STMicroelectronics	STPS1L30A
18	1	F100	20A 250Vac	FUSE BOARD MNT 20A 250VAC 72VDC	Bel Fuse Inc.	0678L9200-02
19	1	FAN100	DC FAN	DC Fans DC Fan, 40x10mm, 12VDC, 7CFM, 0.48W, 20.6dBA, 5800RPM, 0.12inch H2O, Vapo Bearing, MagLev Motor	Sunon	MF40101V2-1000U-A99
20	1	GT100	B88069X0780S102	GDT 540V 5KA THROUGH HOLE	EPCOS (TDK)	B88069X0780S102
21	1	J100	1717033	SCREW TERM BLOCK PCB 3POS 7.5MM GREEN	Phoenix Contact	1717033
22	1	J101	AUX-PS			
23	1	J102	VOUT	SCREW TERM BLOCK PCB 2POS 7.62MM	RS Pro	7901130
24	4	J103 J116 J129 J143	CON10F	CONN RCPT 10POS 0.079 GOLD SMD	Samtec Inc.	CLT-105-02-L-D-BE-A-K-TR
25	48	J104 J105 J106 J107 J108 J109 J110 J111 J112 J113 J114 J115 J117 J118 J119 J120 J121 J122 J123 J124 J125 J126 J127 J128 J130 J131 J132 J133 J134 J135 J136 J137 J138 J139 J140 J141 J144 J145 J146 J147 J148 J149 J150 J151 J152 J153 J154 J155	CON1	ZERO PROFILE RECEPTACLE WITH EAR	Mill-Max Manufacturing Corp.	0640-0-15-15-48-27-10-0
26	1	J142	con70-2x35-strip-female	CONN HEADER FEMALE .100 DUAL STR 70POS	SAMTEC	SSW-135-01-F-D

Item	Q.ty	Ref.	Part/Value	Description	Manufacturer	Order code
27	1	L100	2x4.5mH	CMC 4.5MH 18A 2LN TH	Wurth Electronics Inc.	7448051804
28	3	L101 L102 L103	1891.0010	PFC INDUCTOR 1891 SERIES	MAGNETICA	1891.0010
29	3	M100 M101 M102	HF	HF HALF BRIDGE MODULES		
30	1	M103	LF	LF HALF BRIDGE MODULE		
31	6	N1 N2 N3 N4 N5 N6	NUT M3	HEX NUT 0.217" NYLON M3	Keystone Electronics	4688
32	1	Q100	STS6NF20V, SO-8	MOSFET N-CH 20V 6A 8SOIC	STMicroelectronics	STS6NF20V
33	1	Q101	STS6NF20V, SO-8	MOSFET N-CH 20V 6A 8SOIC	STMicroelectronics	STS6NF20V
34	4	Q102 Q103 Q104 Q105	STR2N2VH5, SOT-23	MOSFET N-CH 20V 2.3A SOT-23	STMicroelectronics	STR2N2VH5
35	3	R100 R101 R102	330k	RES 330K OHM 5% 1/4W 1206	YAGEO	RC1206JR-07330KL
36	1	R103	150	RES 150 OHM 5W 5% RADIAL	TE Connectivity Passive Product	SQMW5150RJ
37	8	R104 R186 R187 R188 R189 R190 R194 R195	10k	RES SMD 10K OHM 1% 1/10W 0603	Yageo	RC0603FR-0710KL
38	6	R105 R106 R107 R108 R114 R115	470k	RES SMD 470K OHM 1% 1/4W 1206	Yageo	RC1206FR-07470KL
39	1	R109	1k	RES SMD 1K OHM 1% 1/10W 0603	Yageo	RC0603FR-071KL
40	1	R110	0	RES SMD 0 OHM JUMPER 1/8W 0805	Yageo	RC0805JR-070RL
41	1	R111	33K	RES SMD 33K OHM 1% 1/10W 0603	Yageo	RC0603FR-0733KL
42	1	R112	0	RES SMD 0 OHM JUMPER 1/8W 0805	Yageo	RC0805JR-070RL
43	2	R113 R116	11k	RES SMD 11K OHM 0.1% 1/10W 0603	Panasonic Electronic Components	ERA-3AEB113V
44	14	R117 R118 R129 R130 R133 R135 R136 R137 R150 R151 R166 R167 R182 R183	10	RES SMD 10 OHM 0.1% 1/10W 0603	Bourns Inc.	CRT0603-BY-10R0ELF
45	3	R119 R121 R124	1M	RES 1M OHM 1% 1/4W 1206	YAGEO	RC1206FR-071ML
46	1	R120	6m	RES 0.006 OHM 1% 3W 2512	Panasonic Electronic Components	ERJ-MS4HF6M0U
47	2	R122 R123	100	RES SMD 100 OHM 0.1% 1/10W 0603	Yageo	RT0603BRD07100RL
48	1	R125	20k	RES SMD 20K OHM 0.1% 1/10W 0603	Yageo	RT0603BRD0720KL

Item	Q.ty	Ref.	Part/Value	Description	Manufacturer	Order code
49	2	R126 R127	1.5k	RES SMD 1.5K OHM 0.1% 1/10W 0603	Yageo	RT0603BRD071K5L
50	2	R128 R131	75k	RES SMD 75K OHM 0.1% 1/10W 0603	Panasonic Electronic Components	ERA-3AEB753V
51	1	R132	1k	RES SMD 1K OHM 1% 1/10W 0603	Yageo	RC0603FR-071KL
52	1	R134	33K	RES SMD 33K OHM 1% 1/10W 0603	Yageo	RC0603FR-0733KL
53	15	R138 R146 R147 R148 R152 R154 R162 R163 R164 R168 R170 R178 R179 R180 R184	10k	RES SMD 10K OHM 0.1% 1/10W 0603	Panasonic Electronic Components	ERA-3AEB103V
54	3	R139 R155 R171	47k	RES SMD 47K OHM 1% 1/10W 0603	Yageo	RC0603FR-0747KL
55	16	R140 R144 R149 R153 R156 R160 R165 R169 R172 R176 R181 R185 R191 R192 R193 R196	0	RES 0 OHM JUMPER 1/10W 0603	YAGEO	RC0603FR-070RL
56	3	R141 R157 R173	100	RES SMD 100 OHM 1% 1/10W 0603	Yageo	RC0603FR-07100RP
57	3	R142 R158 R174	0	CHIP RESISTOR SMD 1% 1/10W 0603	YAGEO	RC0603FR-070RL
58	3	R145 R161 R177	10k	RES SMD 10K OHM 1% 1/10W 0603	Yageo	RC0603FR-0710KL
59	1	RL100	250Vac-16A	RELAY GEN PURPOSE SPDT 16A 18V	TE Connectivity Potter & Brumfield Relays	RT314018
60	1	RT100	16	ICL 16 OHM 20% 1.7A 8.5MM	EPCOS (TDK)	B57153S0160M000
61	4	RV100 RV101 RV102 RV103	S14K385E2K1	VARISTOR 620V 6KA DISC 14MM	EPCOS (TDK)	B72214P2381K101
62	6	S4 S5 S6 S7 S8 S9	SPACER M3x20	HEX STANDOFF M3 NYLON 20MM	Keystone Electronics	25505
63	7	T100 T101 T102 T103 T104 T105 T106	B82801B0504A050	CURR SENSE XFMR 1:50 SMD	EPCOS - TDK Electronics	B82801B0504A050
64	1	U100	TSV911ILT	IC OPAMP GP 8MHZ RRO SOT23-5	STMicroelectronics	TSV911ILT
65	4	U101 U102 U105 U108	ACHS-7122-000E	HALL EFFECT IC LF	Broadcom Limited	ACHS-7122-000E
66	3	U103 U106 U109	LMV358IDT, SO-8	Low cost, low power, input/output rail-to-rail operational amplifiers	STMicroelectronics	LMV358IDT
67	3	U104 U107 U110	TSV911AILT, SOT23-5L	IC OPAMP GP 1 CIRCUIT SOT23-5	STMicroelectronics	TSV911AILT

Item	Q.ty	Ref.	Part/Value	Description	Manufacturer	Order code
68	4	Y100 Y101 Y102 Y103	2.2nF	CAP CER 2200PF 250VAC RADIAL	Murata Electronics North America	DE2E3KY222MA3BM02F

Table 5. **Control board bill of materials**

Item	Q.ty	Ref.	Part/Value	Description	Manufacturer	Order code
1	1	C300	4.7uF	CAP CER 4.7UF 16V X5R 0805	Wurth Electronics Inc.	885012107013
2	21	C301 C302 C303 C304 C305 C306 C307 C308 C309 C312 C321 C323 C324 C331 C336 C346 C348 C349 C350 C351 C352	0.1uF	CAP CER 0.1UF 25V X7R 0603	Würth Elektronik	885012206071
3	3	C310 C313 C347	1 uF	CAP CER 1UF 16V X7R 0603	Wurth Electronics Inc.	885012206052
4	2	C311 C332	10000pF	CAP CER 10000PF 25V X7R 0603	Würth Elektronik	885012206065
5	2	C314 C315	4.3pF	CAP CER 4.3PF 50V C0G/NP0 0603	Murata Electronics	GRM1885C1H4R3CA01D
6	2	C316 C325	8pF	CAP CER 8PF 50V C0G/NPO 0603	Yageo	CC0603DRNPO9BN8R0
7	1	C317	470pF	CAP CER 470PF 25V C0G/NP0 0603	Würth Elektronik	885012006042
8	4	C319 C322 C326 C353	22pF	CAP CER 22PF 25V C0G/NP0 0603	Würth Elektronik	885012006034
9	1	C320	10uF	CAP CER 10UF 16V X5R 0805	Wurth Electronics Inc.	885012107014
10	5	C333 C338 C339 C340 C341	0.22uF	CAP CER 0.22UF 25V X7R 0603	Würth Elektronik	885012206073
11	2	C334 C335	1000pF	CAP CER 1000PF 25V C0G/NP0 0603	Würth Elektronik	885012006044
12	4	C342 C343 C344 C345	22pF	CAP CER 22PF 25V C0G/NP0 0603	Würth Elektronik	885012006034
13	2	D300 D301	BAS70-05FILM, SOT23	DIODE ARRAY SCHOTTKY 70V SOT23-3	STMicroelectronics	BAS70-05FILM
14	3	D302 D303 D304	BAS70-05FILM, SOT23	DIODE ARRAY SCHOTTKY 70V SOT23-3	STMicroelectronics	BAS70-05FILM
15	1	D306	RED 2mA	LED RED DIFFUSED 0603 SMD	OSRAM Opto Semiconductors Inc.	LS L29K-G1J2-1-Z
16	1	D307	YELLOW 2mA	LED YELLOW DIFFUSED 0603 SMD	OSRAM Opto Semiconductors Inc.	LY L29K-J1K2-26-Z
17	1	D308	GREEN 2mA	LED GREEN DIFFUSED 0603 SMD	OSRAM Opto Semiconductors Inc.	LG L29K-G2J1-24-Z
18	2	J300 J304	con3-strip-male	CONN HEADER VERT 3POS 2.54MM	Amphenol ICC (FCI)	68001-203HLF

Item	Q.ty	Ref.	Part/Value	Description	Manufacturer	Order code
19	1	J301	con70-2x35-strip-male-R/A	CONN HEADER R/A 70POS 2.54MM	Amphenol ICC (FCI)	68020-172HLF
20	1	J302	CONN 10	CONN HEADER SMD 10POS 1.27MM	Samtec Inc.	FTSH-105-01-L-DV-K-TR
21	1	J303	con4-strip-male	CONN HEADER .100 STR 4POS	Amphenol ICC (FCI)	68001-204HLF
22	1	JP1	SHORT	2 PIN SHORTED TO CONNECT DIFFERENT NETS		
23	1	L300	600Ohm@100MHz	FERRITE BEAD 600 OHM 0603 1LN	Wurth Electronics Inc.	742863160
24	10	R301 R302 R328 R334 R338 R341 R342 R343 R352 R413	0	RES 0 OHM JUMPER 1/10W 0603	YAGEO	RC0603FR-070RL
25	1	R303	*	CHIP RESISTOR SMD 1% 1/10W 0603		
26	5	R304 R329 R330 R331 R332	10k	RES SMD 10K OHM 1% 1/10W 0603	Yageo	RC0603FR-0710KL
27	1	R305	470	RES 470 OHM 1% 1/10W 0603	YAGEO	RC0603FR-10470RL
28	6	R307 R308 R320 R321 R372 R374	0	0 OHM JUMPER 0603	YAGEO	RC0603FR-070RL
29	14	R309 R310 R377 R378 R381 R382 R385 R386 R389 R390 R393 R394 R397 R398	10k	RES SMD 10K OHM 0.1% 1/10W 0603	Panasonic Electronic Components	ERA-3AEB103V
30	7	R311 R353 R354 R355 R356 R357 R358	100	RES SMD 100 OHM 1% 1/10W 0603	Yageo	RC0603FR-07100RP
31	3	R313 R314 R315	1k	RES SMD 1K OHM 1% 1/10W 0603	Yageo	RC0603FR-071KL
32	1	R316	75	RES 75 OHM 1% 1/10W 0603	YAGEO	RC0603FR-0775RL
33	4	R326 R336 R339 R344	100K	RES SMD 100K OHM 1% 1/10W 0603	Yageo	RC0603FR-07100KL
34	5	R327 R337 R340 R345 R409	1k	RES SMD 1K OHM 1% 1/10W 0603	Yageo	RC0603FR-071KL
35	5	R359 R360 R361 R362 R363	680	RES 680 OHM 1% 1/10W 0603	YAGEO	RC0603FR-10680RL
36	2	R373 R375	0	0 OHM JUMPER 0603	YAGEO	RC0603FR-070RL
37	12	R376 R379 R380 R383 R384 R387 R388 R391 R392 R395 R396 R399	15k	RES SMD 15K OHM 0.1% 1/10W 0603	Panasonic Electronic Components	ERA-3AEB153V

Item	Q.ty	Ref.	Part/Value	Description	Manufacturer	Order code
38	4	R400 R401 R402 R403	1.5k	RES SMD 1.5K OHM 0.1% 1/10W 0603	Yageo	RT0603BRD071K5L
39	4	R404 R405 R406 R407	3k	RES SMD 3K OHM 0.1% 1/10W 0603	Panasonic Electronic Components	ERA-3AEB302V
40	1	R408	100K	RES SMD 100K OHM 1% 1/10W 0603	Yageo	RC0603FR-07100KL
41	1	SW300	Switch-WE-430483025816	SWITCH TACTILE SPST-NO 0.05A 12V	Wurth Electronics Inc.	430483025816
42	15	TP300 TP301 TP304 TP308 TP311 TP314 TP323 TP324 TP325 TP326 TP327 TP331 TP332 TP333 TP334	5001	TEST POINT PC MINI .040"D BLACK	Keystone Electronics	5001
43	1	U205	STLM20W87F, SOT323-5L	SENS TEMP ANLG VOLT SOT-323-5	STMicroelectronics	STLM20W87F
44	1	U300	STM32G474QET6, LQFP 128 14x14x1.4 mm	MAINSTREAM ARM CORTEX-M4 CORE WI	STMicroelectronics	STM32G474QET6
45	3	U302 U305 U306	TSV912IDT, SO-8	IC OPAMP GP 8MHZ RRO 8SO	STMicroelectronics	TSV912IDT
46	3	U303 U304 U307	TSV911ILT, SOT23-5L	IC OPAMP GP 8MHZ RRO SOT23-5	STMicroelectronics	TSV911ILT
47	1	U308	LMV321RILT, SOT23-5L	IC OPAMP GP 1 CIRCUIT SOT23-5	STMicroelectronics	LMV321RILT
48	1	Y300	32.768kHz	CRYSTAL 32.7680KHZ 12.5PF SMD	CTS-Frequency Controls	TFE322P32K7680R
49	1	Y301	24MHz	CRYSTAL 24.0000MHZ 9PF SMD	IQD Frequency Products	LFXTAL071177REEL

Table 6. Auxiliary power supply board bill of materials

Item	Q.ty	Ref.	Part/Value	Description	Manufacturer	Order code
1	1	C1	1nF	CAP CER 1000PF 760VAC Y5U RADIAL	Vishay BC Components	VY1102M35Y5UG63V0
2	1	C3	220pF	CAP CER 220PF 1KV C0G/NP0 1206	Murata Electronics	GRM31A5C3A221JW01D
3	3	C6 C10 C19	10uF	CAP CER 10UF 35V X5R 0805	Murata Electronics	GRM21BR6YA106KE43K
4	3	C7 C26 C28	220uF	CAP ALUM 220UF 20% 16V RADIAL	Wurth Electronics Inc.	860020373010
5	1	C9	0.1uF	CAP FILM 0.1UF 20% 305VAC RADIAL	EPCOS (TDK)	B32921C3104M000

Item	Q.ty	Ref.	Part/Value	Description	Manufacturer	Order code
6	1	C13	1000pF	CAP CER 1000PF 25V C0G/NP0 0603	Würth Elektronik	885012006044
7	1	C14	33nF	CAP CER 0.033UF 25V X7R 0603	Würth Elektronik	885012206068
8	2	C15 C24	0.1uF	CAP CER 0.1UF 50V X7R 0603	Würth Elektronik	885012206095
9	1	C18	1uF	CAP CER 1UF 50V X7R 0805	Würth Elektronik	885012207103
10	2	C22 C23	10uF	10 µF Tantalum Capacitors 16 V 0805 20%	KYOCERA AVX	F981C106MSUAJ6
11	1	C25	22uF	CAP ALUM 22UF 20% 400V RADIAL	Rubycon	400PX22MEFCG412.5X20
12	1	C27	22nF	CAP CER 0.022UF 25V X7R 0603	Würth Elektronik	885012206067
13	1	D1	STPS6M100DEE, PowerFLAT&#8482	DIODE SCHOTTKY 100V 6A POWERFLAT	STMicroelectronics	STPS6M100DEE-TR
14	1	D2	800V 2.2A	BRIDGE RECT 1PHASE 800V 2.2A YBS	Taiwan Semiconductor Corporation	YBS2206G RAG
15	1	D3	STTH1R06A, SMA	DIODE GEN PURP 600V 1A SMA	STMicroelectronics	STTH1R06A
16	2	D4 D6	BAT41ZFILM, SOD-123	DIODE SCHOTTKY 100V 200MA SOD123	STMicroelectronics	BAT41ZFILM
17	1	D7	18V	DIODE ZENER 18V 500MW SOD80	Vishay Semiconductor Diodes Division	BZT55C18-GS08
18	1	D8	STPS1L60A	DIODE SCHOTTKY 60V 1A SMA	STMicroelectronics	STPS1L60A
19	1	F2	2.5A 250V	FUSE BRD MNT 250VAC/ 125VDC SMD	Littelfuse Inc.	047602.5MR
20	1	ISO1	SFH6106-2T	OPTOISOLATOR 5.3KV TRANS 4-SMD	Vishay Semiconductor Opto Division	SFH6106-2T
21	1	J2	CON2	CONN HEADER R/A 2POS 5.08MM	Samtec Inc.	TSW-202-08-T-S-RA
22	1	J4	CON4	CONN HEADER R/A 4POS 2.54MM	Samtec Inc.	TSW-104-08-T-S-RA
23	1	L2	3.3uH	FIXED IND 3.3UH 4.7A 25 MOHM TH	Wurth Electronics Inc.	7447462033
24	2	R2 R3	100k	RES 100K OHM 5% 1/4W 1206	YAGEO	RC1206JR-07100KL
25	1	R5	0	RES 0 OHM JUMPER 1/4W 1206	YAGEO	RC1206JR-070RL
26	1	R6	4.7	RES 4.7 OHM 5% 1/4W 1206	YAGEO	RC1206JR-074R7L
27	1	R14	620k	RES 620K OHM 1% 1/10W 0603	YAGEO	RC0603FR-07620KL
28	1	R15	82k	RES 82K OHM 1% 1/10W 0603	YAGEO	RC0603FR-0782KL
29	1	R16	22k	RES SMD 22K OHM 1% 1/10W 0603	Yageo	RC0603FR-0722KL

Item	Q.ty	Ref.	Part/Value	Description	Manufacturer	Order code
30	1	R17	33K	RES SMD 33K OHM 1% 1/10W 0603	Yageo	RC0603FR-0733KL
31	1	R18	3.9	RES 3.9 OHM 1% 1/10W 0603	YAGEO	RC0603FR-073R9L
32	1	R19	1k	RES SMD 1K OHM 1% 1/10W 0603	Yageo	RC0603FR-071KL
33	1	R20	100K	RES SMD 100K OHM 1% 1/10W 0603	Yageo	RC0603FR-07100KL
34	1	R21	200k	RES 200K OHM 1% 1/10W 0603	YAGEO	RC0603FR-07200KL
35	1	R22	130k	RES 130K OHM 1% 1/10W 0603	YAGEO	RC0603FR-07130KL
36	1	R23	15k	RES SMD 15K OHM 1% 1/10W 0603	Yageo	RC0603FR-0715KL
37	1	R24	12k	RES 12K OHM 5% 1/8W 0805	YAGEO	RC0805JR-0712KL
38	1	T1	750319460R01	TRANSFORMER REV.01	WURTH ELEKTRONIK	750319460
39	1	U1	LD29080DT50R	IC REG LINEAR 5V 800MA DPAK	STMicroelectronics	LD29080DT50R
40	1	U2	VIPER35LD, SO-16	IC OFFLINE SWITCH FLYBACK 16SO	STMicroelectronics	VIPER35LD
41	1	U3	LD29080S33R, SOT-223	IC REG LINEAR 3.3V 800MA SOT223	STMicroelectronics	LD29080S33R (Contact our sales office)
42	1	U4	TS432ILT, SOT23	IC VREF SHUNT 10V 1% SOT23-3	STMicroelectronics	TS432ILT

Table 7. High-frequency half-bridge board bill of materials

Item	Q.ty	Ref.	Part/Value	Description	Manufacturer	Order code
1	5	C1 C3 C6 C9 C13	0.1uF	CAP CER 0.1UF 50V X7R 0603	Würth Elektronik	885012206095
2	5	C2 C4 C8 C10 C14	1uF	CAP CER 1UF 50V X7R 0805	Würth Elektronik	885012207103
3	2	C5 C11	*	CAPACITOR CERAMIC SMD 0603		
4	2	C7 C12	100pF	CAP CER 100PF 50V C0G/NP0 0603	Würth Elektronik	885012006057
5	12	J1 J2 J3 J4 J5 J7 J8 J9 J10 J11 J12 J13	CON1	CONN PC PIN CIRC 0.040DIA GOLD	Mill-Max Manufacturing Corp.	3301-2-14-21-00-00-08-0
6	1	J6	CON10	CONN HEADER SMD R/A 10POS 2MM	Amphenol ICC (FCI)	10112690-G03-05ULF
7	1	Q1	STR2N2VH5, SOT-23	MOSFET N-CH 20V 2.3A SOT-23	STMicroelectronics	STR2N2VH5
8	2	Q2 Q3	STW70N60DM6, TO-247	MOSFET N-CH 600V 62A TO247	STMicroelectronics	STW70N60DM6
9	2	R1 R2	10k	RES SMD 10K OHM 1% 1/10W 0603	Yageo	RC0603FR-0710KL

Item	Q.ty	Ref.	Part/Value	Description	Manufacturer	Order code
10	1	R3	0	RES SMD 0 OHM JUMPER 1/8W 0805	Yageo	RC0805JR-070RL
11	2	R4 R11	*	CHIP RESISTOR SMD 1% 1/10W 0603		
12	2	R5 R12	22	RES 22 OHM 5% 1/4W 1206	YAGEO	RC1206JR-0722RL
13	1	R6	0	RES SMD 0 OHM JUMPER 1/8W 0805	Yageo	RC0805JR-070RL
14	4	R7 R9 R13 R15	0	RES 0 OHM JUMPER 1/10W 0603	YAGEO	RC0603FR-070RL
15	2	R8 R14	4.7	RES 4.7 OHM 5% 1/4W 1206	YAGEO	RC1206JR-074R7L
16	2	R10 R16	6.8k	RES 6.8K OHM 1% 1/10W 0603	YAGEO	RC0603FR-076K8L
17	1	U1	ISE1212A	DC DC CONVERTER 12V 1W	XP Power	ISE1212A
18	2	U2 U3	STGAP2SM, SO-8	DGTL ISO 4A single Gate Drive	STMicroelectronics	STGAP2SMTR

Table 8. **Low-frequency half-bridge board bill of materials**

Item	Q.ty	Ref.	Part/Value	Description	Manufacturer	Order code
1	5	C1 C3 C6 C9 C13	0.1uF	CAP CER 0.1UF 50V X7R 0603	Würth Elektronik	885012206095
2	5	C2 C4 C8 C10 C14	1uF	CAP CER 1UF 50V X7R 0805	Würth Elektronik	885012207103
3	2	C5 C11	*	CAPACITOR CERAMIC SMD 0603		
4	2	C7 C12	100pF	CAP CER 100PF 50V C0G/NP0 0603	Würth Elektronik	885012006057
5	12	J1 J2 J3 J4 J5 J7 J8 J9 J10 J11 J12 J13	CON1	CONN PC PIN CIRC 0.040DIA GOLD	Mill-Max Manufacturing Corp.	3301-2-14-21-00-00-08-0
6	1	J6	CON10	CONN HEADER SMD R/A 10POS 2MM	Amphenol ICC (FCI)	10112690-G03-05ULF
7	1	Q1	STR2N2VH5, SOT-23	MOSFET N-CH 20V 2.3A SOT-23	STMicroelectronics	STR2N2VH5
8	2	Q2 Q3	STY145N65M5, Max247	MOSFET N-CH 650V 138A MAX247	STMicroelectronics	STY145N65M5
9	2	R1 R2	10k	RES SMD 10K OHM 1% 1/10W 0603	Yageo	RC0603FR-0710KL
10	1	R3	0	RES SMD 0 OHM JUMPER 1/8W 0805	Yageo	RC0805JR-070RL
11	2	R4 R11	*	CHIP RESISTOR SMD 1% 1/10W 0603		
12	2	R5 R12	1k	RES 1K OHM 5% 1/4W 1206	YAGEO	RC1206JR-101KL
13	1	R6	0	RES SMD 0 OHM JUMPER 1/8W 0805	Yageo	RC0805JR-070RL

Item	Q.ty	Ref.	Part/Value	Description	Manufacturer	Order code
14	4	R7 R9 R13 R15	0	RES 0 OHM JUMPER 1/10W 0603	YAGEO	RC0603FR-070RL
15	2	R8 R14	33	RES 33 OHM 5% 1/4W 1206	YAGEO	RC1206JR-0733RL
16	2	R10 R16	6.8k	RES 6.8K OHM 1% 1/10W 0603	YAGEO	RC0603FR-076K8L
17	1	U1	ISE1212A	DC DC CONVERTER 12V 1W	XP Power	ISE1212A
18	2	U2 U3	STGAP2SM, SO-8	DGTL ISO 4A single Gate Drive	STMicroelectronics	STGAP2SMTR

9 Custom evaluation boards information

Notice: *This/These evaluation board(s) is/are custom designed and built according to specific requests from customer (You) and is/are destined for evaluation and testing of ST products in a research and development setting.*

By using or installing (as applicable) this evaluation kit you accept all the terms of the EVALUATION BOARD TERMS OF USE available at: www.st.com/epla.

10 Regulatory compliance information

Notice for US Federal Communication Commission (FCC)

For evaluation only; not FCC approved for resale

FCC NOTICE - This kit is designed to allow:

(1) Product developers to evaluate electronic components, circuitry, or software associated with the kit to determine

whether to incorporate such items in a finished product and

(2) Software developers to write software applications for use with the end product.

This kit is not a finished product and when assembled may not be resold or otherwise marketed unless all required FCC equipment authorizations are first obtained. Operation is subject to the condition that this product not cause harmful interference to licensed radio stations and that this product accept harmful interference. Unless the assembled kit is designed to operate under part 15, part 18 or part 95 of this chapter, the operator of the kit must operate under the authority of an FCC license holder or must secure an experimental authorization under part 5 of this chapter 3.1.2.

Notice for Innovation, Science and Economic Development Canada (ISED)

For evaluation purposes only. This kit generates, uses, and can radiate radio frequency energy and has not been tested for compliance with the limits of computing devices pursuant to Industry Canada (IC) rules.

À des fins d'évaluation uniquement. Ce kit génère, utilise et peut émettre de l'énergie radiofréquence et n'a pas été testé pour sa conformité aux limites des appareils informatiques conformément aux règles d'Industrie Canada (IC).

11 References

[1] STMicroelectronics STM32G474xB/C/E Arm® Cortex®-M4 32-bit MCU+FPU, 170MHz / 213 DMIPS, 128 KB SRAM, rich analog, math acc, 184ps 12 chan Hi-res time, Datasheet - production data.

[2] M. Torrisi, S. Messina and M. Cacciato, "Hysteresis Current Control for a High efficiency totem pole PFC in zero voltage switching," 2021 23rd European Conference on power Electronics and Applications (EPE'21 ECCE Europe), 2021, pp. P.1-P.10, doi:10.23919/EPE21ECCEEurope50061.2021.9570441.

[3] STMicroelectronics STY145N65M5 N-channel 650V, 0.012 Ω typ., 138 A MDmesh™ M5 - Datasheet.

[4] STMicroelectronics, Application Note, AN2761, “Solution for designing a transition mode PFC pre-regulator with the L6562A”.

[5] STMicroelectronics STW70N60DM6 N-channel 600 V, 36 mΩ typ., 62 A, MDmesh DM6 power MOSFETs - Datasheet.

[6] STMicroelectronics, eDesignSuite page for ZVS Totem-Pole PFC: ZVS Totem-Pole PFC.

Revision history

Table 9. Document revision history

Date	Version	Changes
08-Nov-2023	1	Initial release.
22-Mar-2024	2	Updated Section 6: EMI test results.

Contents

List of figures

List of tables